RANGE EXPANSION OF AN EXOTIC ASIAN SNAIL (MELANOIDES TUBERCULATA) INTO CENTRAL TEXAS RIVERS, AND THE PARASITOLOGICAL CONSEQUENCES THEREOF

by

Stephen Forrest Harding, B.S.

A thesis submitted to the Graduate Council of
Texas State University in partial fulfillment
of the requirements for the degree of
Master of Science
with a Major in Aquatic Resources
December 2016

Committee Members:

David Huffman, Chair

David Rodriguez

Jacob Jackson

FAIR USE AND AUTHOR'S PERMISSION STATEMENT

Fair Use

Duplication Permission

DEDICATION

First and foremost, I would like to dedicate this work to my fiancée and family. Their support provided me with the motivation needed to enter into the master's program and continue my education. For this I will be forever grateful and I am lucky to have you all in my life.

ACKNOWLEDGEMENTS

First, I would like to acknowledge my advisor, Dr. David G. Huffman for extending to me the opportunity to work under his tutelage and continue my education. These past two years were among the most challenging I have endured in my life thus far and I will always cherish them. I appreciate your advice, honesty, open nature, and patience when encountering my lack of experience. For this, I am forever indebted to you.

I would also like to acknowledge my committee members, Dr. David Rodriguez and Dr. Jacob Jackson for their support during this time. I firmly believe that I would not have been able to complete this project without it. I also appreciate the guidance and help I received from you both. I genuinely thank you and look forward to working with you gentlemen in the future.

Finally, I would like to acknowledge everyone who helped with work in the lab and field collections. Their names are as follows: Evan Valenta, Mclean Worsham, James D. Evans, Cassandra P. Mccumber-Aguilar, Angel M. Peltola, Carlos Baca, Jeremiah Leach, Dakota L. Rhoad, Amanda C. Andrews, Gabriella D. Solis, Thomas Marshall, Nick Porter and Jube Guajardo. The help you all provided was valuable and much appreciated.

TABLE OF CONTENTS

Page

LIST OF TABLES

Table **Page**

LIST OF FIGURES

Figure **Page**

ABSTRACT

The invasive gastropod *Melanoides tuberculata* (Thiaridae) has been established in Texas since the 1960's (Murray, 1964). For decades, sensitivity of these snails to cold winter temperatures restricted reproducing populations of the snail to thermally stable waters (Fleming 2002, Rader *et al*., 2003, Mitchell and Brandt, 2005). The mechanisms driving this expansion are not yet understood but parasitic consequences of this phenomenon are such that the invasive Asiatic trematodes *Centrocestus formosanus*, *Haplorchis pumilio*, and *Philophthalmus gralli* are likely to follow their snail hosts into novel habitats from which they were previously excluded. Non-Metric Multidimensional Analysis was used as a distance based comparison of phenotypic characteristics in attempt to qualitatively partition morphometric variation observed within and among several Texas snail populations. Snails exhibiting unique combinations of phenotypic characters were subject to molecular analyses using primers targeting the mitochondrial 16s rRNA gene. Genetic analyses revealed pockets of genetic variation within and among the studied populations. Genetic diversity of local snail populations was placed into a global context using 16s rRNA sequence data available from GenBank. Additionally, geometric estimates of conch morphology were used to further partition subtle variation via multivariate analyses. This dual perspective is a starting point for future studies investigating niche preferenda and genetic diversity of *M. tuberculata* populations established in the United States.

I. INTRODUCTION

Natural History of *M. tuberculata*

Melanoides tuberculata has been described as a usually polyploid and sometimes aneuploid species that usually reproduces parthenogenetically (Jacob, 1958). Males are rare in most populations or nonexistent in some (Livshits et al., 1984). Parthenogenetic reproduction is one of the factors that make the species a successful invader. Dumping an aquarium containing a single female can establish a colony of genetically identical individuals (representing one genotypic clone) in a novel environment. If the aquarium contains several snails purchased at different times or from differing sources, the invasive colony may contain two or more clonal genotypes. Polyploidy renders the molecular genetics particularly difficult to study, because there may be anywhere between one and hypothetically six alleles present at a particular locus in an individual, depending on which genotypic clone the individual represents.

Prior to 2000, as many as 16 different genotypic clones of *M. tuberculata* were described (Pointier 1989, Samadi et al. 1999) and assigned a unique two- or three-letter identification code based on the initials of the locality where first found. Facon et al. (2003) found additional genotypes, including hybrids, and developed a presumptive phylogenetic tree of the clones using 12S and 16S rRNA mitochondrial genes. Four clades were found among the clones (Facon et al. 2003): one representing the invasion of the Caribbean and Venezuela from Africa, the Middle East, and the Indian Ocean; a second representing the invasion of Polynesia; a third having invaded Colombia from an

unknown source; and the fourth clade having invaded continental America from Southeast Asia.

Critical thermal limits and thermal preferenda

Reports have suggested that the critical thermal limits for *M. tuberculata* established in Texas are between 17 and 32 °C (Mitchell and Brandt 2005). Another independent study found that the snail is restricted to placid or low velocity water flow with temperatures between 18° and 30°C (Rader *et al*., 2003). However, the thermal preferenda of *M. tuberculata* obtained from a pet store in Ohio ranged between 15.8 and 20.6 °C (Gerald and Spezzano 2005), and these snails were reported to avoid temperatures above 21.2 °C. These observations establish speculated dissimilarity in lethal thermal tolerances.

Global Range Expansion of Melanoides tuberculata

Circumtropical expansion

Melanoides tuberculata (Gastropoda: Thiaridae) is now commonly found in circumtropical freshwaters and some brackish waters. The species is native to Old World tropics and has invaded many areas of the New World tropics. The date of the first introduction of *M. tuberculata* into the western hemisphere is unknown, but the snail was most likely introduced via the aquarium trade (Murray 1971). It was reported to have established breeding populations in the continental U.S. as early as 1964 (Murray and Woopschall 1965), Panama by 1971 (Abbott 1973), Mexico by 1973 (Abbott 1973), West Indies by 1978 (Pointier et al. 1993), Cuba by 1981 (Perera et al. 1990), and Brazil

by 1986 (Vaz et al. 1986). Globally, the snail has been detected in tropical climates all over the world (Facon et al., 2003).

Nearctic expansion

Melanoides tuberculata has also invaded temperate regions wherever waters with tropical characteristics may be found; especially geothermally warmed or thermally stable springs with thermal minima higher than 17 °C. In the continental USA, they have now been reported in multiple spring-fed systems from western, north western and southern states (Benson and Neilson 2015, Karatayev et al. 2009, Murray 1975, Rader et al. 2003, Wingard et al. 2008).

Introductions of *M. tuberculata* into Texas Waters

The first reports of *M. tuberculata* in Texas were from the headwaters of the San Antonio River, Bexar County and from Landa Lake in New Braunfels, Comal County (Murray 1964). The species was subsequently detected in the Comal River in 1964, (Murray and Woopschall 1965). *M. tuberculata* was not detected in the San Marcos River (SMR) by Murray and Woopschall (1965) but was presumed to be present. In 1973, *M. tuberculata* shells comprised the main component of a gravel bar in the San Marcos River just upstream from the mouth of Sessom Creek (D.G. Huffman, pers. comm.) and was later reported to be abundant and widespread in the reaches upstream from Thompson's Island in 1978 (Lindholm 1979); thus, the snail was probably introduced to the SMR sometime shortly after 1964 but before 1973. *Melanoides tuberculata* has since been reported to inhabit many thermally stable springs throughout Texas (United States Geological Survey 2015).

Range Expansion of Thiarids in Texas

Range expansion of Melanoides tuberculata in the Guadalupe River

Until 2009, the known distribution of *M. tuberculata* in Central Texas was restricted to thermally stable spring runs, and it did not survive winters in connecting surface-fed streams owing to lethal winter temperatures (Fleming 2002). In 2000 & 2001, three searches for *M. tuberculata* in the Guadalupe River near its confluence with the Comal River yielded only a few empty shells that had probably washed downstream from the Comal River (Fleming 2002). A subsequent search by Dr. David Huffman's lab in 2009 yielded snails thriving in the Guadalupe River up to 2 km downstream from the confluence, and in 2012, mature live snails several years old (> 50 mm) were found thriving in the Guadalupe River approximately 15 km downstream from the Comal River. Temperature profiles (Figure 1) show water temperatures had remained well below 18° C for 36 consecutive days during the prior winter. During that same cold period, the ambient water temperature had cooled to as low as 12 °C. These data serve as evidence of thermal ambience at these sites.

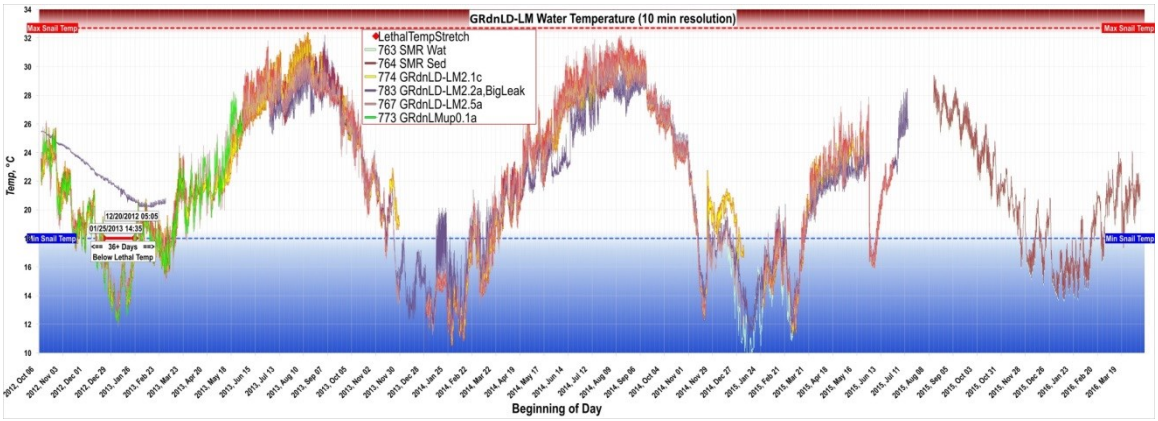

Figure 1: Seasonal variation in water temperature obtained from HOBO data loggers for the Guadalupe River and Lower San Marcos River (Station SMR 13). There are four data loggers in the Guadalupe River and two in the lower San Marcos River. Of the two in the lower SMR, one is suspended in water column close to the benthos and the other is buried approximately 15 cm into the benthos. The graphic also displays the experimentally observed lethal thermal maximum in red (32ºC) and lethal thermal minimum in blue (18ºC). Temperature data reveals water temperatures fluctuating below the minimum for extended periods of time. All data collected by Dr. David G. Huffman and Stephen Forrest Harding.

Range expansion of Melanoides tuberculata in the San Marcos River

Reports of *M. tuberculata* in the Upper SMR indicate that the species was well established there in the 1970's. However, population density has now substantially decreased in the Upper SMR for unknown reasons. Until recently, the snail had never been reported to occur in the SMR downstream from the A. E. Wood Fish Hatchery (<3 river km downstream from the headwaters). However, in 2014, abundant live *M. tuberculata* were discovered to be thriving in the lower SMR as far as 50+ river km downstream from the headsprings in thermally ambient water (Figure 2).

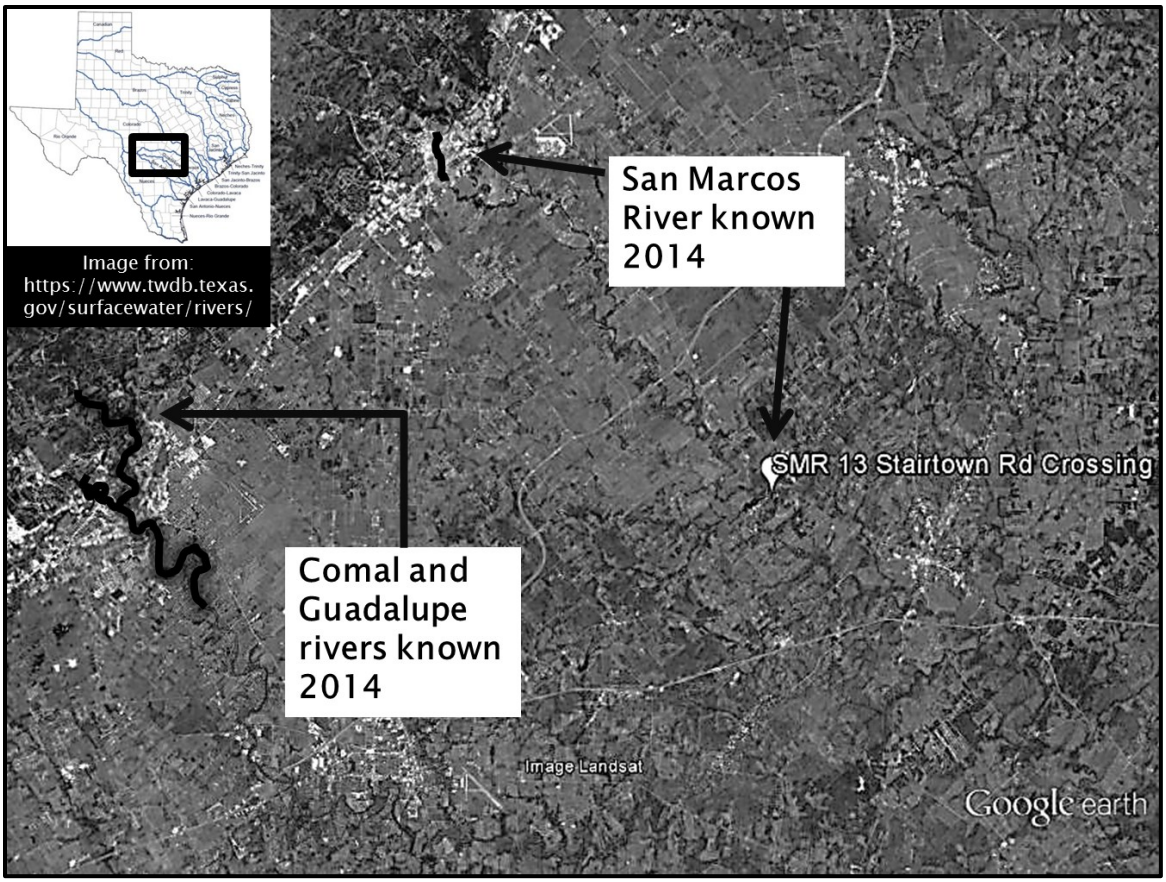

Figure 2: Known distribution of *M. tuberculata* in the Comal, the Guadalupe and the San Marcos rivers as of 2014. Darkened lines on the map represent the distributions of M. tuberculata within these rivers. The pin symbol represents a population discovered at site SMR13 which is approximately 50 river km downstream from the headwaters. This population was well outside previously known *M. tuberculata* distributions for this river. *Source:* 29º44'18.53" N 97º50'47.76" W **Google Earth** December 16, 2015. November 1, 2016

Speculation regarding the range expansion of *M. tuberculata* into colder waters

There are reports of *M. tuberculata* surviving through the winter at some temperate locations by burying in mud (Livshits and Fishelson 1983), and we have recovered snails buried several cm below the benthos in some areas. However, while snails had been reported for decades in the thermally stable Comal River and Upper

SMR, *M. tuberculata* had not been found in the connecting thermally ambient waters until just recently. This suggests that the recent range expansion could possibly be due either to a newly acquired low-temperature tolerance, or to a different introduction of a previously undocumented genotypic clone of *M. tuberculata* with a low-temperature tolerance.

Whatever the case, this previously undocumented strain of *M. tuberculata* may have already spread into other connecting surface waters of Central and South Texas; if so, endemic fishes and gamefishes, once thought to be protected from infection with parasites hosted by the invasive snail, could now be vulnerable to the parasites transmitted by these snails for the first time.

It is not our intent to refute any of findings from previous reports of lethal thermal limits; however, one design element that was overlooked in the cited thermal experiments was the genotype of the experimental snails used in the respective studies. Measurements of the experimental snails were reported, but no attempt was made to determine their geographic origin, or the genotypic clones that were represented.

It seems reasonable to assume that these genotypic clones (or at least the clades), having evolved in differing regions of the world, would have different ecological limits and preferenda. Additionally, within species, ecological and physiological variation may cause differences in trematode susceptibility, as reported for at least two genotypic clones in Lake Malawi (Genner et al. 2007). With such information available for Central Texas clones of *M. tuberculata*, the management issues associated with mitigating the effects of the invasive parasites supported by these snails might be simplified.

Parasitological Ramifications of Thiarid Snail Invasions

Many mollusk species, especially snails, have a unique relationship with a community of parasitic flatworms known as the Trematoda, or flukes. Nearly all trematode species utilize a snail as first intermediate host in their lifecycles, most of which are complex, and usually involve two or three hosts (Haseeb and Fried 1997). *Melanoides tuberculata* is of special concern as they are first intermediate hosts for multiple species of digenetic trematode parasites, several of which are sources of major human health problems in Asia (Pinto and de Melo 2011).

Four exotic trematode species are now known to occur in Texas as a result of having been introduced following the establishment of their exotic thiarid snail hosts. These four trematodes have a high level of host-specificity for their first intermediate snail host, and therefore cannot become established beyond the range of the snails. So, while we are most interested in the deleterious effects the parasites are exerting on native vertebrates (some of which are listed); a key component in any approach to mitigation is the thiarid snails. An understanding of the invasion dynamics of the various genetic clones of these snails is thus a necessary pre-requisite to any study attempting to shed light on management issues pertaining to the parasites.

II. Methods

Study Areas

The Comal River and the upper & lower sections of the San Marcos River were the most intensively sampled drainages. The Guadalupe River was sampled as flow velocities allowed. The San Felipe River (Del Rio, TX), Finnegan Springs (Devils River State Natural Area, TX) and Las Moras Springs (Brackettville TX) were also sampled and chosen because they have established populations of *M. tuberculata* and were easily accessible. GPS coordinates of all sampling sites can be found in Table located in the Appendix. Figure 3 is a map of Texas displaying the distribution of the sampled locations distributed across the state. A map of all sampled locations for the Comal and San Marcos rivers is depicted below (Figure 4).

Figure 3: Map of sampling locations across Texas. Data was plotted using ArcGIS Online platform. *Sources:* Esri, DeLorme, HERE, TomTom, Intermap, increment P Corp., GEBCO, USGS, FAO, NPS, NRCAN, GeoBase, IGN, Kadaster NL, Ordnance Survey, Esri Japan, METI, Esri China (Hong Kong), swisstopo, MapmyIndia, and the GIS User Community.

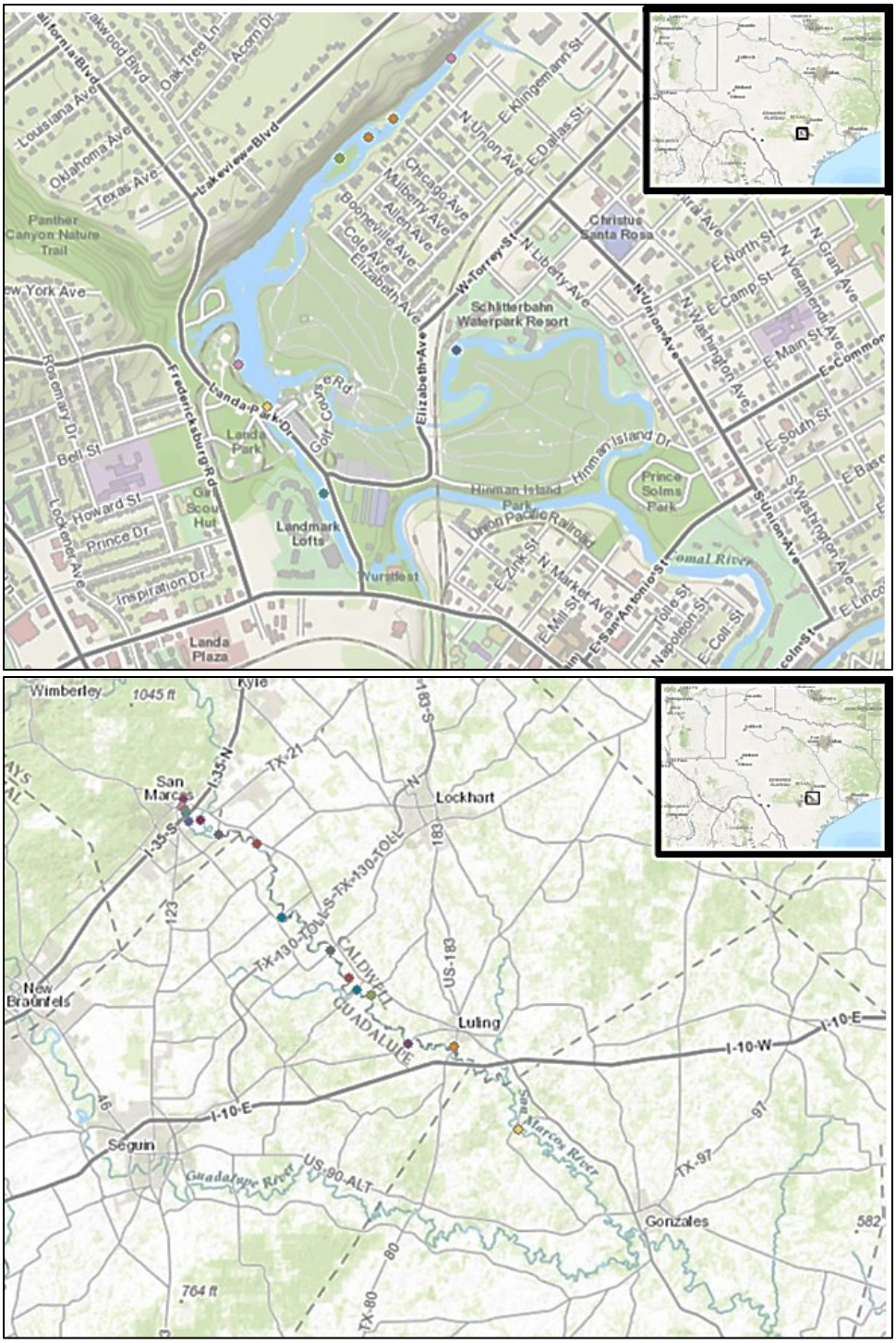

Figure 4: Mapped sample sites for the Comal River (Right) and the San Marcos River (Left). . Data was plotted using ArcGIS Online platform. *Sources:* Esri, DeLorme, HERE, TomTom, Intermap, increment P Corp., GEBCO, USGS, FAO, NPS, NRCAN, GeoBase, IGN, Kadaster NL, Ordnance Survey, Esri Japan, METI, Esri China (Hong Kong), swisstopo, MapmyIndia, and the GIS User Community.

Sampling Protocol

Sampling of shallow water habitats was accomplished using dip nets. The sampling of deeper habitats was done using snorkeling and SCUBA diving techniques. All snails collected were separated into labeled containers corresponding to the site being sampled. Approximately 20 live snails were collected at each sited detected and were promptly transported to our lab where they were maintained in flow-through containers in flowing artesian water until morphometric and genetic analyses were initiated.

Molecular Analyses

DNA isolation and purification

All DNA extractions were initiated using approximately 25 mg of live tissue from the proboscis and foot. The snail tissue was then placed into a sterile 1.8 mL Eppendorf tube. Two protocols were used to isolate and purify genomic DNA during this study.

The first protocol was used on the Comal River snail samples and was conducted by adding 300 µL of cell-lysis solution and 20 µL of proteinase K to the Eppendorf tube containing the snail tissue. The reaction was then shaken and incubated at 55°C until the tissues completely dissolved. After tissues were dissolved, 100 µL of protein precipitation solution was added to the 1.8 mL Eppendorf tubes containing the cell lysate, the resulting solution was vortexed, and then chilled on ice for 5 minutes. After incubation, samples were centrifuged at 21,130 x g for 5 minutes and cooled again for a maximum of 4 minutes after centrifugation. The supernatant was then decanted into a sterile 1.8 mL Eppendorf tube containing 300 µL of 100% isopropanol and centrifuged at 21,130 x g for 5 minutes. After centrifugation, the isopropanol was decanted off and the

precipitated DNA was allowed to dry for approximately 10 minutes. The precipitated DNA was rehydrated using 300 µL of 70% ethanol, shaken and then centrifuged at 21,130 x g for 2 minutes. The ethanol was decanted and DNA was allowed to dry for at least 30 minutes. After drying, 200 µL of Qiagen buffer AE elution buffer was added to the purified DNA and incubated at room temperature overnight.

The second protocol was used on the San Marcos River, San Felipe River, and Las Moras Springs snails and followed the Thermo Scientific GeneJET Genomic DNA Purification Kit Mammalian Tissue and Rodent Tail Genomic DNA Purification Protocol with slight modifications.

Gel electrophoresis

After DNA isolation and purification, all samples were diagnosed for high molecular weight DNA. This diagnosis was carried out using a 1% agarose gel and 0.5x TBE buffer solution. A 5 µL aliquot of purified DNA from each sampled snail was mixed with 3 µL of loading dye and placed into a well in the agarose gel. The electrophoresis reaction was allowed to proceed at 98 volts for 25 minutes. After this time, the gel was viewed under high intensity UV light to determine if high molecular weight DNA was successfully extracted and purified.

PCR amplification

All DNA samples were amplified using standard polymerase chain reaction (PCR) amplification protocols. All snail DNA amplifications were performed using mitochondrial DNA primers that targeted the 16S ribosomal subunit rRNA gene. The primers used for all amplifications were 16SF (5'-TAGCATGAATGGTCTGACGAAAGC-3') and 16SR (5'-

AAGGAGATTATGCTGTTATCCC-3'). All amplifications were performed using 25 µL total volume containing 12.5 µL, 0.25 µL forward primer, 0.25 µL reverse primer and 11.5 µL nuclease free H_2O. The thermal profile used followed the profile proposed by Facon *et al*. (2003) with initial denaturation at 92° for 1 min., then and a final elongation at 68° for 7 mins.

PCR Clean-up and DNA Sequencing

PCR products were cleaned up using the ExoSAP-IT® PCR product clean up protocol (Affymetrix). Both DNA strands were sequenced independently using the following protocol: 0.5 µL BigDye® Terminator v1.1, v3.1 5x Sequencing Buffer (Applied Biosystems Inc.), 1.0 µL BigDye® Terminator v3.1 Cycle Sequencing RR-100 (Applied Biosystems Inc.), 0.12 µL primer and 2.38 µL nuclease free H_2O. Cycle sequencing products were purified using 400 µL Sephadex™ G-50 Superfine (GE Healthcare) gel filtration medium. Purified cycle sequencing products were dehydrated overnight and then incubated in 10-15 µL formamide at 95.0° for 3 mins. Sequencing was conducted using an Applied Biosystems 3500 Genetic Analyzer.

Sequence analysis

All sequence editing, alignments and establishment of phylogenetic relationships was completed using Geneious Pro v5.5.9 Software (http://www.geneious.com, Kearse *et al.,* 2012). Pre-alignment sequence edits were performed to remove the bases flanking the sequences that contained ambiguities that were unresolvable. After this initial edit, de novo contig assemblies were created for each individual snail using the forward and reverse sequences for the respective snail sample. This de novo assembly allowed for

finer scale editing of ambiguous bases within the 16S sequence without confounding the sequence caused by an alignment with other non-edited sequences. After all ambiguities were resolved, consensus sequences were generated for each snail. The 16S primer sequences were then assembled to the consensus sequences to remove the primer regions flanking the 16S sequence leaving a total contig length of 249 bp data matrix. Consensus sequences were aligned using a ClustalW algorithm (Thompson *et al.,* 1994; Facon *et al.,* 2003).

Phylogenetic Analysis

Phylogenetic relationships were established using neighbor-joining (NJ) methodologies executed in PAUP* portable version 4.0b10 (Swafford 2003). Sequence evolution models were tested using MODELTEST integrated into the PAUP* geneious plugin. MODELTEST results indicated the HKY85 + Γ evolutionary model fits the data best. This model was used to build the NJ and ML trees and contained the parameters: base frequencies (A= 0.3690, C = 0.1324, G = 0.1742, T = 0.3244), Transition/Transversion Ratio (2.3822; kappa = 5.5124709) and distribution of rates at variable sites = gamma (continuous) with an alpha shape parameter (0.3059). Maximum parsimony (MP) and maximum likelihood (ML) topologies were established using CIPRES Science Gateway (Miller *et al*., 2010). Bootstrap methodology was used to evaluate nodal stability with 1000 replicates for NJ, ML and MP topologies. Maximum Likelihood outputs were visualized using T-REX webserver (Boc et al., 2012). Maximum Parsimony output was visualized using Geneious. Bayesian inferences were obtained using MrBayes v3.2.6 (Huelsenbeck & Ronquist, 2001) Geneious plugin.

Morphometric Analyses

Digitizing the Shell

Prior to initiation of genetic analyses, the snails were cleaned, assigned an accession number, and photographed using a Casio EX-FH26 digital camera with a macro lens. Prior to photographing, the snails were pressed into a block of modeling clay with the columellar axis parallel to a horizontal plane, and with the shell rotated on its columellar axis such that the camera is looking straight down into the anal sulcus. Each photograph included a millimeter ruler in the field of view for calibration purposes. Bright daylight LED lights were arrayed with one at the apex and one on each side of the snail to minimize shadows. The camera-assigned sequence number for the photograph was associated with the accession number assigned to the snail.

Qualitative Analysis

Phenotypes of *M. tuberculata* have been characterized in previous studies using distinct features of the conch such as color patterns (ornamentation) and sculpture. This methodology provides a foundation to qualitatively assess differences in phenotypic variation. Qualitative assessment of phenotypic variation in snail shells from this study was captured using distance based rank scoring methodologies employed first by Samadi *et al.,* (1999); then further modified (Facon *et al.,* 2003; Van Bocxlaer *et al.,* 2015). Non-applicable or ambiguous qualitative variables in published data were eliminated from the data matrix. A total of 14 morphological characters were scored for this assessment (Table 1). Ranks within a qualitative variable were determined by DGH and SFH using

progressive based systematics. For example, background shell coloration varied from very pale to dark, therefore a rank of 1 was assigned to very pale and 4 for dark.

Rank scores for all snails characterized by qualitative variables were Z-transformed to stabilize the variance among disproportionate variable scores and used to construct a distance matrix ordinated using non-metric Multi-dimensional Scaling (nMDS) analyses using 15 dimensions. A Euclidean distance method was used to accommodate for missing ranks when snails did not exhibit a particular qualitative trait. R version 3.3.1 and packages Vegan v.2.4-1 and MASS 7.3-45 were used to execute the analyses.

Quantitative Analysis

The utility of using a geometric morphometric approach to exploring subtle variation of shell morphology has been established to be viable (Gustafson et al., 2014). Using the photographs mentioned earlier, precise measurements and angle determinations were obtained using Digimizer Image Analysis software (www.digimizer.com). An array of 40 raw morphometric variables assumed to capture much of the observed conchological variation was measured on the shells (Figure 17, Figure 18, & Figure 19; see Appendix section). The raw variables were then used to derive 56 additional variables, most of which were ratios standardized to total length.

To avoid issues with downstream collinearity, most of the raw variables measured were excluded from final analyses. Only raw metrics estimating the number of whorls, width of the 6^{th} whorl, length of the 6^{th} whorl, and the roundness of the opercular aperture were chosen among the raw variable set. The collinearity of all chosen variables was

tested using a Pearson's correlation matrix and groups of variables with correlations ≥ 0.80 were simplified to one of the correlated variables. Principal Components Analysis (PCA) and Linear Discriminant Functions Analysis (LDFA) were used to select key variables from among the tested variables that captured the majority of variation in shell morphology. Both multivariate analyses were carried out using R version 3.3.1 and the MASS 7.3-45 package.

III. RESULTS

Current Distributional Status of *M. tuberculata* in Central Texas

Multiple live snails were collected at all locations sampled in the Comal River. Efforts in the San Marcos yielded multiple live snails at every site sampled down to the Highway 90 crossing in Luling, Texas (SMR14). The SMR6 and SMR7 sites were not publicly accessible and therefore not sampled. Only empty *M. tuberculata* shells were collected past the SMR 14 site. Sampling efforts in the Guadalupe River yielded no live snails. A map of the speculated, historical and observed contemporary ranges for *M. tuberculata* in central Texas is depicted below (Figure 5). Multiple live snails were collected at all sites in the San Felipe River, Finnegan Springs and Fort Clark Springs localities (See Table in Appendix for gps coordinates).

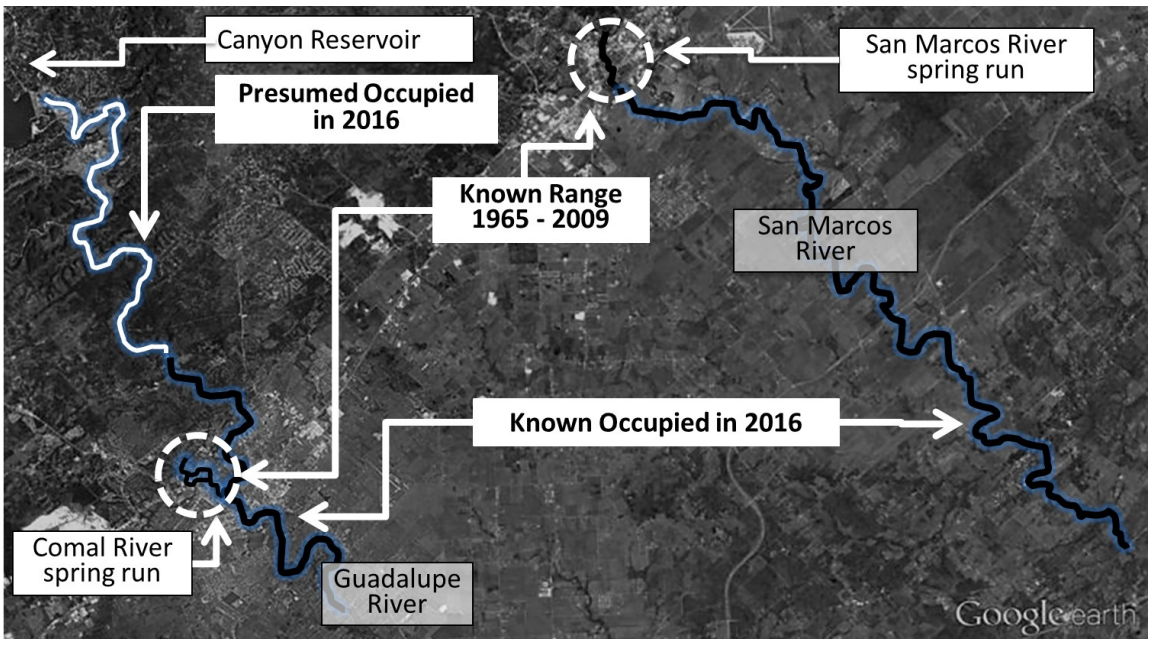

Figure 5: Map showing the historical, contemporary and speculated distributional range for *M. tuberculata* in central Texas. Even though snails were not detected in the Guadalupe River during this study, this range is still valid as there are preserved collections of snails from these localities. Range is valid until future studies can confirm their extirpation from these habitats. *Source:* 29º43'50.73" N 97º54'31.59" W **Google Earth** May 5, 2016. November 1, 2016

Molecular Analyses

Genetic variation and haplotype distribution

Among all snails analyzed, a subset from each sample site was taken and used in genetic analyses. A total of 205 samples were sequenced. There were three haplotypes detected across all sampled locations. Henceforth they are labelled TEX, LSMR, and OCCR. Haplotype labelling convention follows previously published data using acronyms based on the location from which the snail was collected. The most abundant haplotype was the TEX haplotype and was detected across multiple sampling localities except in the SMR at sites below SMR5. The next most abundant was the LSMR haplotype which was found from SMR8 and down to SMR14. There was one individual of the LSMR haplotype found in the Old Channel sampling site located in the Comal River. The rarest haplotype detected was the OCCR haplotype and was only detected in the Old Channel site.

The TEX haplotype is diverged from the LSMR haplotype by 32 bp and from OCCR haplotype by 34 bp (Figure 6). The LSMR and OCCR haplotypes are diverged from each other by 5 bp. Figure 7 and Figure 8 show the distribution of the three haplotypes relative to the sampling localities across Texas. The TEX haplotype was the only haplotype detected among the Big Bend region sites. All three haplotypes were observed in the Comal River, however only the TEX haplotype was detected outside of the Old Channel site. Only the TEX and LSMR haplotypes were observed in the San Marcos River.

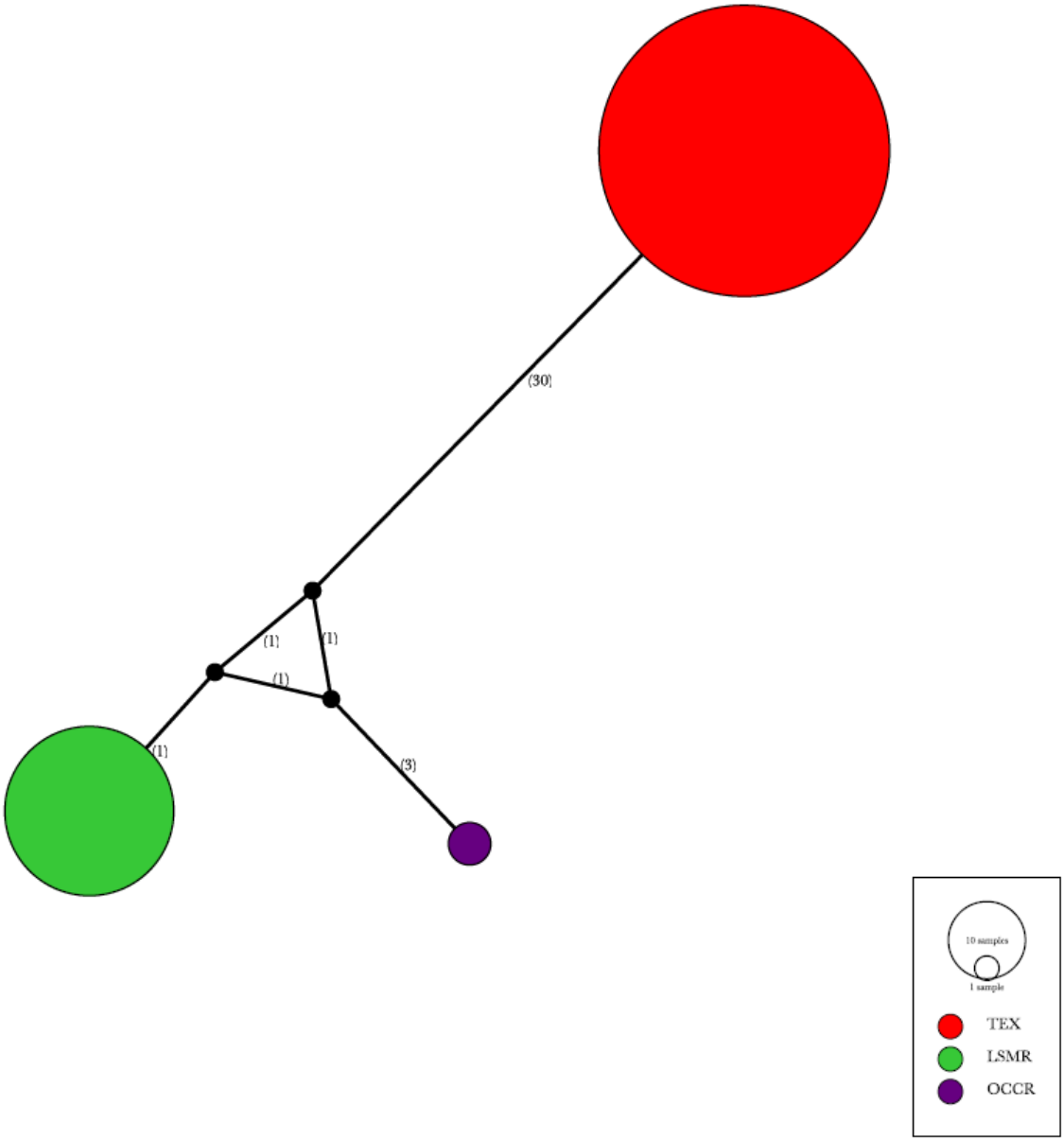

Figure 6: Haplotype network visualizing the divergence observed among collected haplotypes. The numbers in the parenthesis represent the number of base pair mutations between the haplotypes. The black nodes not listed in the legend represent hypothetical haplotypes in between the representative haplotypes.

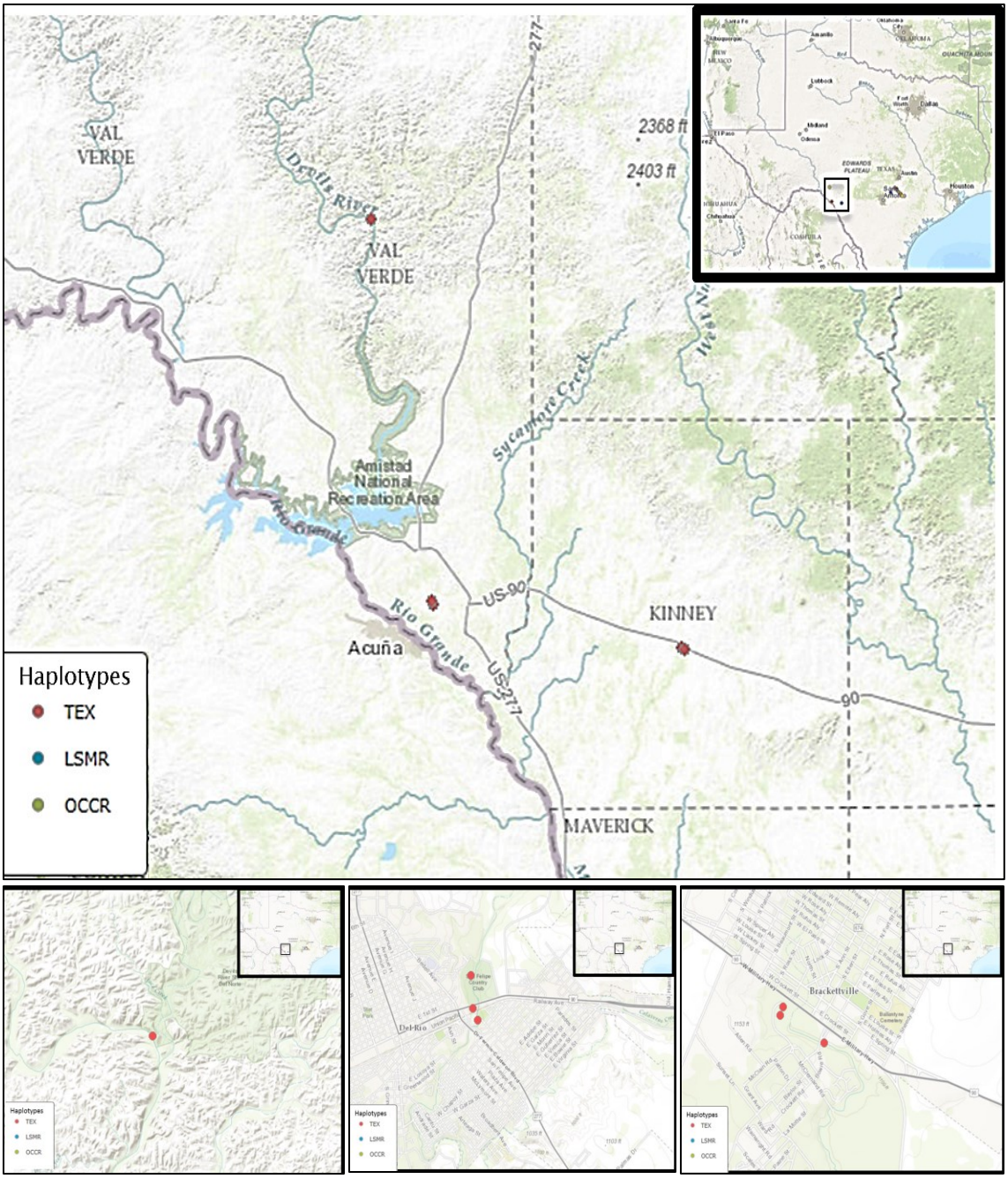

Figure 7: Maps depicting haplotype distribution among the sampling sites in the Big Bend region of Texas. The three smaller maps depict the haplotype distribution within the rivers sampled in this region. The Finnegan Springs site is left, the San Felipe River is middle, and the Fort Clark Springs site is on the right. There was only one location sampled at Finnegan Springs, three locations along the San Felipe River, and three locations at Fort Clark Springs. The TEX haplotype was the only haplotype detected at these sites. Data was plotted using ArcGIS Online platform. *Sources*: Esri, DeLorme, HERE, TomTom, Intermap, increment P Corp., GEBCO, USGS, FAO, NPS, NRCAN, GeoBase, IGN, Kadaster NL, Ordnance Survey, Esri Japan, METI, Esri China (Hong Kong), swisstopo, MapmyIndia, and the GIS User Community.

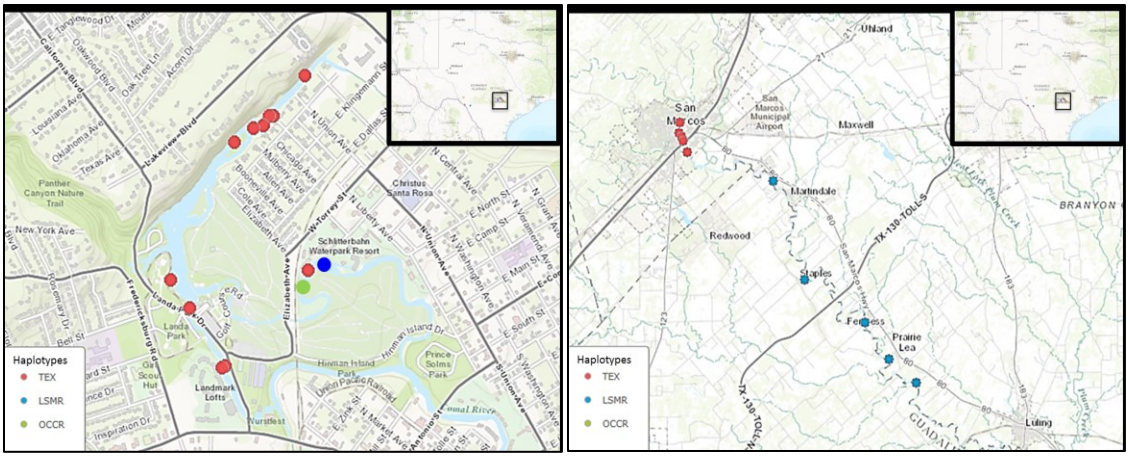

Figure 8: Map depicting haplotype distribution within and among the sampling sites located in the central Texas region. The map on the left shows the observed haplotype distribution in the Comal River. The map on the right shows the observed distribution along the San Marcos River. There were three haplotypes detected in the Comal River and two haplotypes detected in the San Marcos River. Data was plotted using ArcGIS Online platform. *Sources*: Esri, DeLorme, HERE, TomTom, Intermap, increment P Corp., GEBCO, USGS, FAO, NPS, NRCAN, GeoBase, IGN, Kadaster NL, Ordnance Survey, Esri Japan, METI, Esri China (Hong Kong), swisstopo, MapmyIndia, and the GIS User Community.

Phylogenetic Analyses

Phylogenetic inferences reveal the TEX haplotype to be the most highly divergent among the *M. tuberculata* haplotypes collected. The clade containing TEX shows to be more closely related to *Melanoides amabilis* than the other *M. tuberculata* haplotypes collected in this study. Terminal nodes on NJ tree show high bootstrap support. In contrast, some terminal nodes on the Bayesian inference show low bootstrap support. Both Trees are in agreement for established phylogenetic relationships among the Texas snails. Maximum Likelihood reconstruction topology varies from the NJ and Bayesian inferences however, the relationships among the Texas haplotypes are consistent with the other phylogenetic inferences. There is considerably less bootstrap support for Terminal nodes on the Maximum Likelihood inference. All phylogenetic reconstructions support

previously published results that establish *M. tuberculata* as polyphyletic and highly divergent (Facon *et al*., 2003; Van Bocxlaer *et al*., 2015).

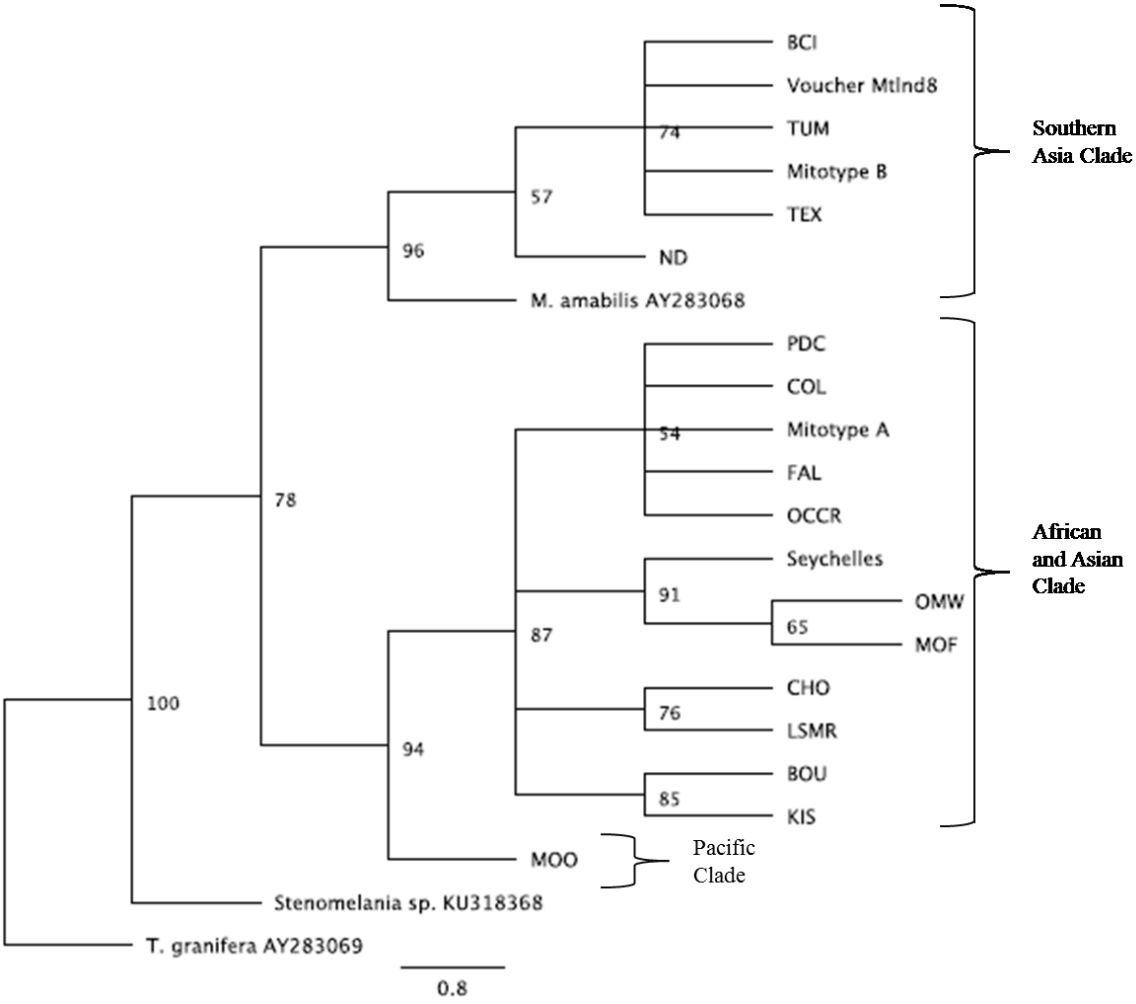

Figure 9: Neighbor Joining phylogenetic tree exhibiting the relationship of Texas *M. tuberculata* among global data accessed into GenBank. Support for tree topology and nodal stability was tested using Bootstrapped analyses with 1000 replicates. Clades designations are reported from Facon et al., (2003). The TEX haplotype falls into the Southern Asian clade. The LSMR and OCCR haplotypes fall into the African and Asian clades. Scale bar at the bottom represents the number of nucleotide substitutions per site.

Figure 10: Illustrated above is the Bayesian inference of phylogeny. Topology varies from the NJ tree, however there is agreement in the relationships of the TEX, LSMR and OCCR haplotypes. Scale bar at the bottom represents the expected number of nucleotide changes per site.

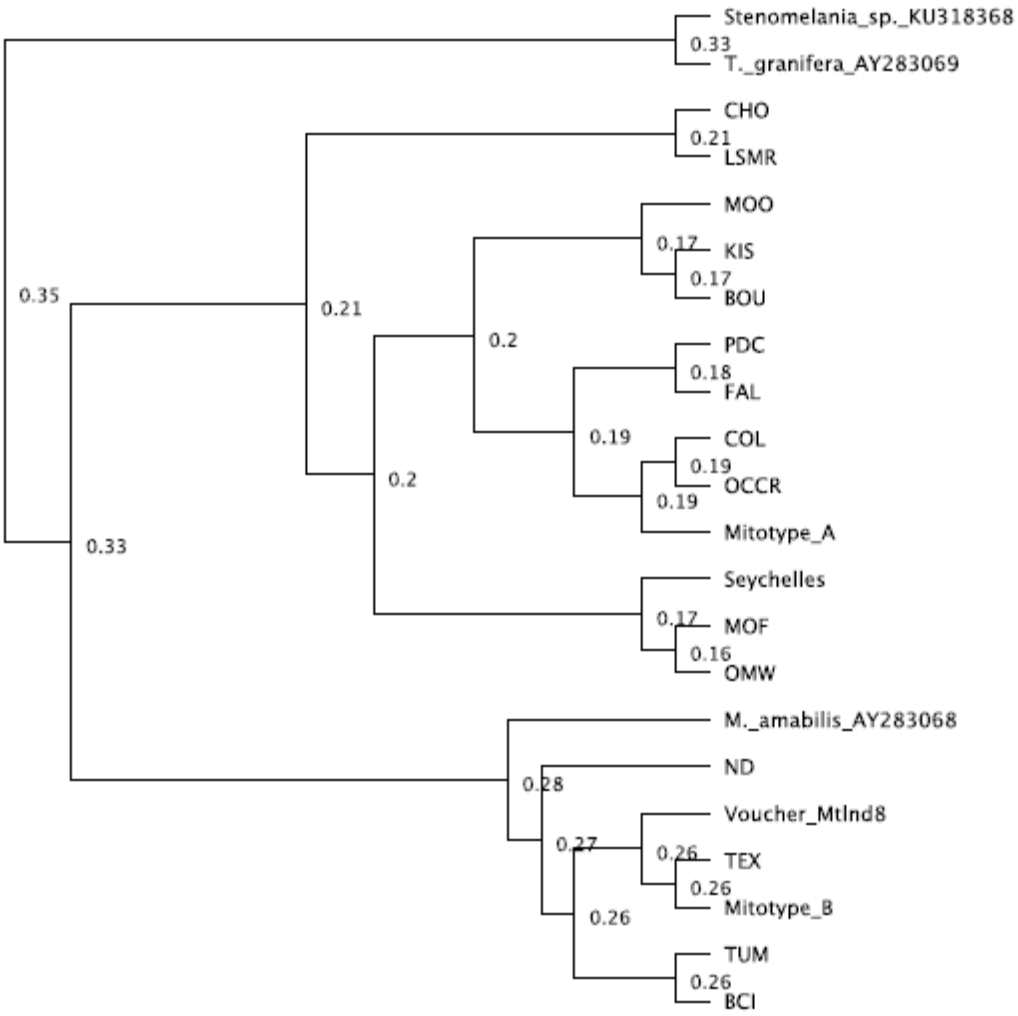

Figure 11: Illustrated above is a Maximum Likelihood estimate of phylogenetic relationships. Topology varies from other trees but the relationships observed between the TEX, LSMR and OCCR haplotypes are consistent with the other phylogenetic reconstructions.

Morphometric Analyses

Qualitative analysis

Among the snails examined 51 unique phenotypical variants were identified (Table 1). Few snails displayed unique characters that provided unambiguous assignment to a phenotype. Despite this ambiguity, there were several phenotypes that were

sufficiently differentiated enough to show clear phenotypic separation, namely snails from the Upper San Marcos River (USMR), Lower San Marcos River (LSMR), Comal River (CR), San Felipe River (SF), and Fort Clark Springs (FCS) (Figure 12). Only the LSMR and OCCR haplotypes displayed deep U-shaped grooves with reticulate ridge patterns inside the grooves and the LSMR haplotype appears to consistently distinct, phenotypically, among all snails collected.

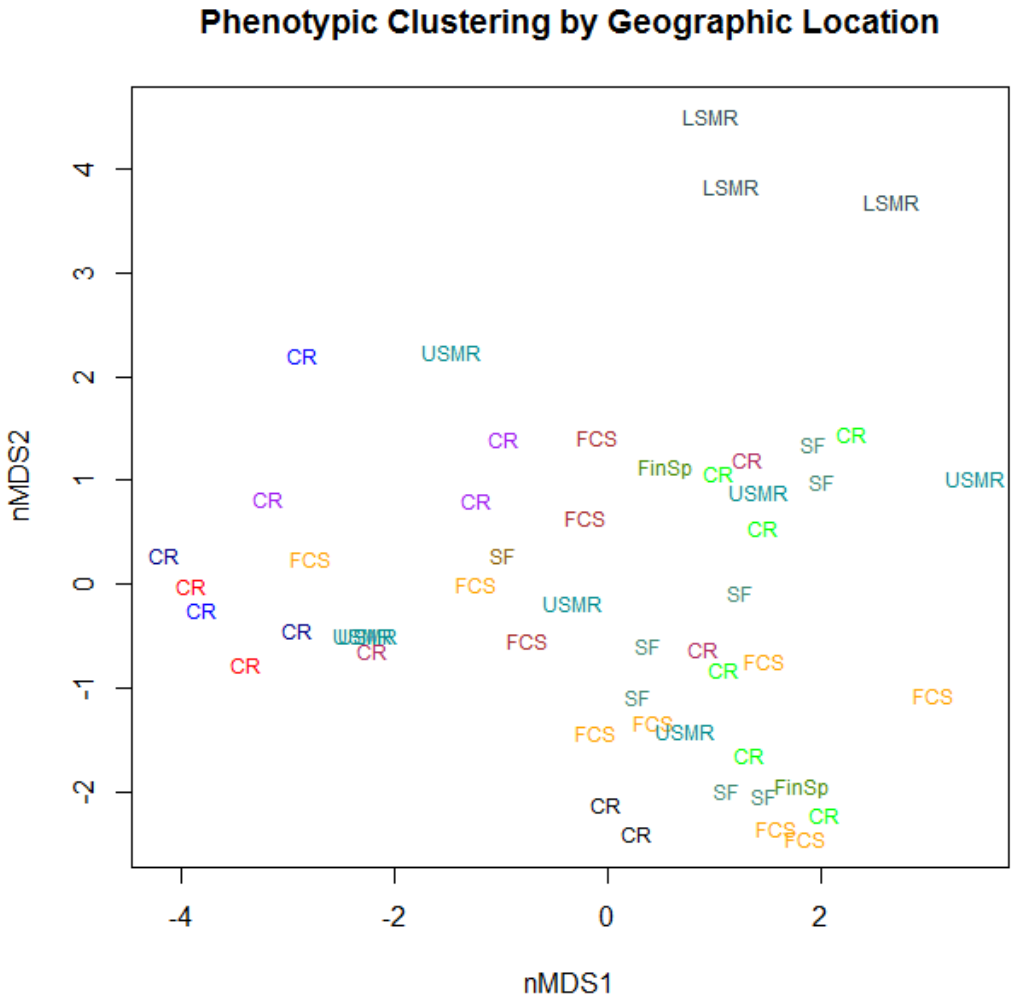

Figure 12: Non-metric Multidimensional Scaling plot showing relationship of qualitative morphological variables among all Texas snails relative to river and sample site (Stress level = 0.0075). Each color represents a different sampling site. Despite being from different geographic localities, there is considerable overlap in qualitative characters. However there is evident morphological differentiation.

When morphological characters were associated with haplotype, aside from one individual, the LSMR haplotype maintained phenotypic separation from the other haplotypes. The distances in qualitative rank scores among the haplotypes were visualized via plotted output of the nMDS analysis (Figure 13). The OCCR haplotype is nested inside a cluster that extends toward the dimension containing the LSMR haplotypes. Photographs of unique phenotypes collected from all the rivers are depicted below (Figure 14).

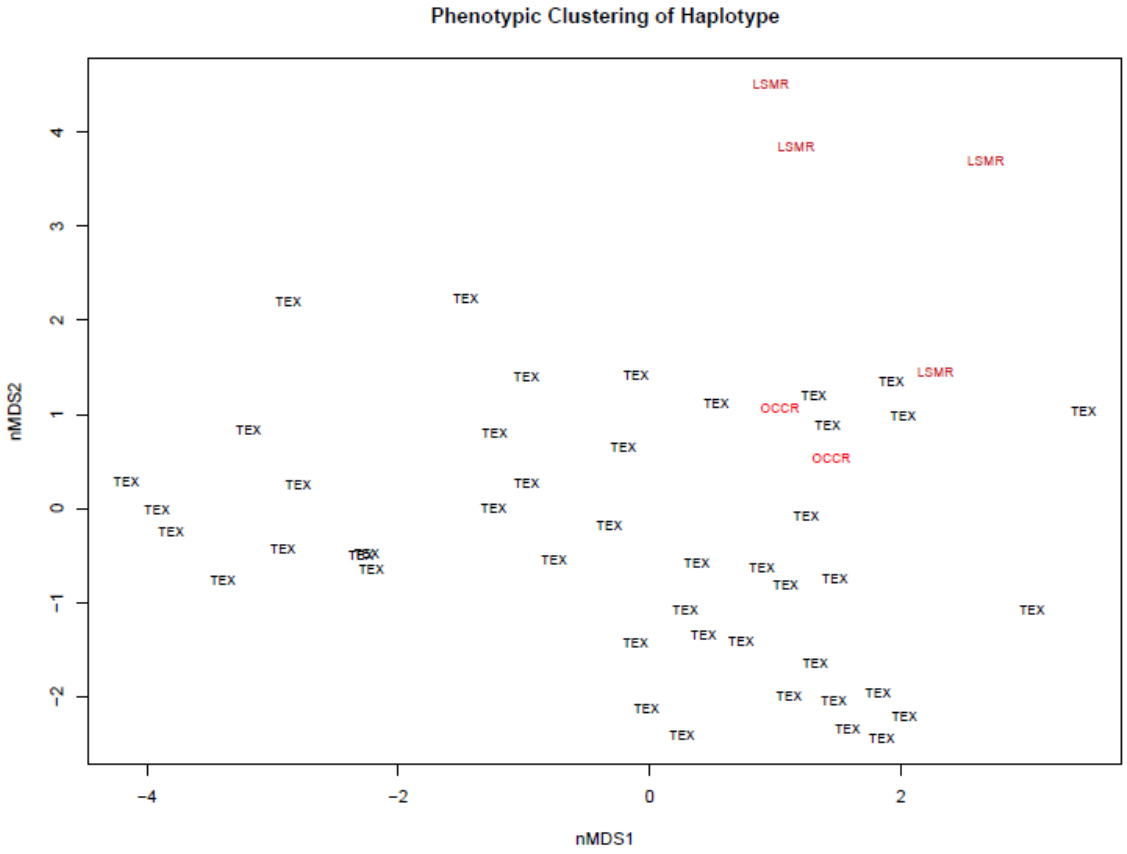

Figure 13: Non-metric Multidimensional Scaling plot showing relationship of qualitative morphological characteristics among all Texas snails collected relative to their associated haplotype (Stress level = 0.0075).

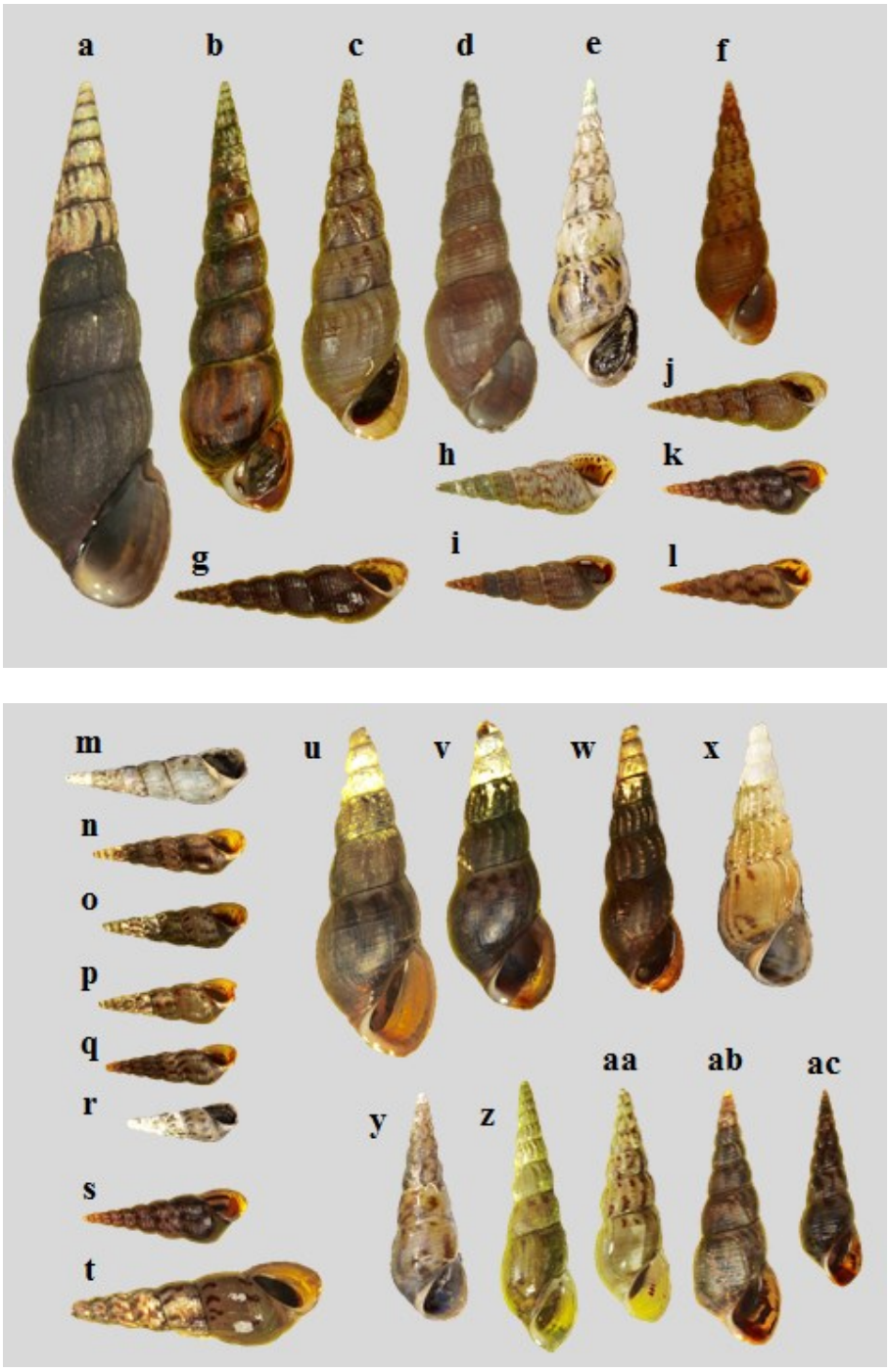

Figure 14: Above are images of collected snails displaying the range of phenotypic variation among all the *M. tuberculata* collected during this study. Letters a-h and j-l correspond to snails collected from the San Marcos and Comal rivers, letter i was only detected in the Old channel site in the Comal River. Letters m-r correspond to snails collected from the San Felipe River. Letters s-t correspond to snails from Finnegan Springs and letters u-ac correspond to snails from Fort Clark Springs. Sizes among snails are to scale. All photographs taken by Stephen F. Harding

Quantitative Analysis

Principal Components Analysis

Results from principal components analysis indicate that the 1st component explained 29.60% of the variation in the data set, component 2 explained 20.72%, component 3 explained 12.90%, and component 4 explained 7.85% for a total of 71.07% of the variation. After several successive iterations of analysis to remove superfluous variables, 24 variables of the original 46 tested variables were retained. Bartlett's test of sphericity was significant ($\chi^2=\infty$; df= 276; $p< 0.05$) suggesting that the variables are not orthogonal, however the n:p ratio is 7.65. Kaiser-Meyer-Olkin test for sampling adequacy score was 0.5, which is lower than the generally accepted value of 0.6, suggesting there are too many variables relative to the number of samples in the data. Based on these criteria, it is open to interpretation whether or not PCA can be efficiently performed on this data set. Despite the aforementioned concerns there are three distinct clusters that correlate to haplotype (Figure 15). Variable loadings are listed in Table (see TABLES section).

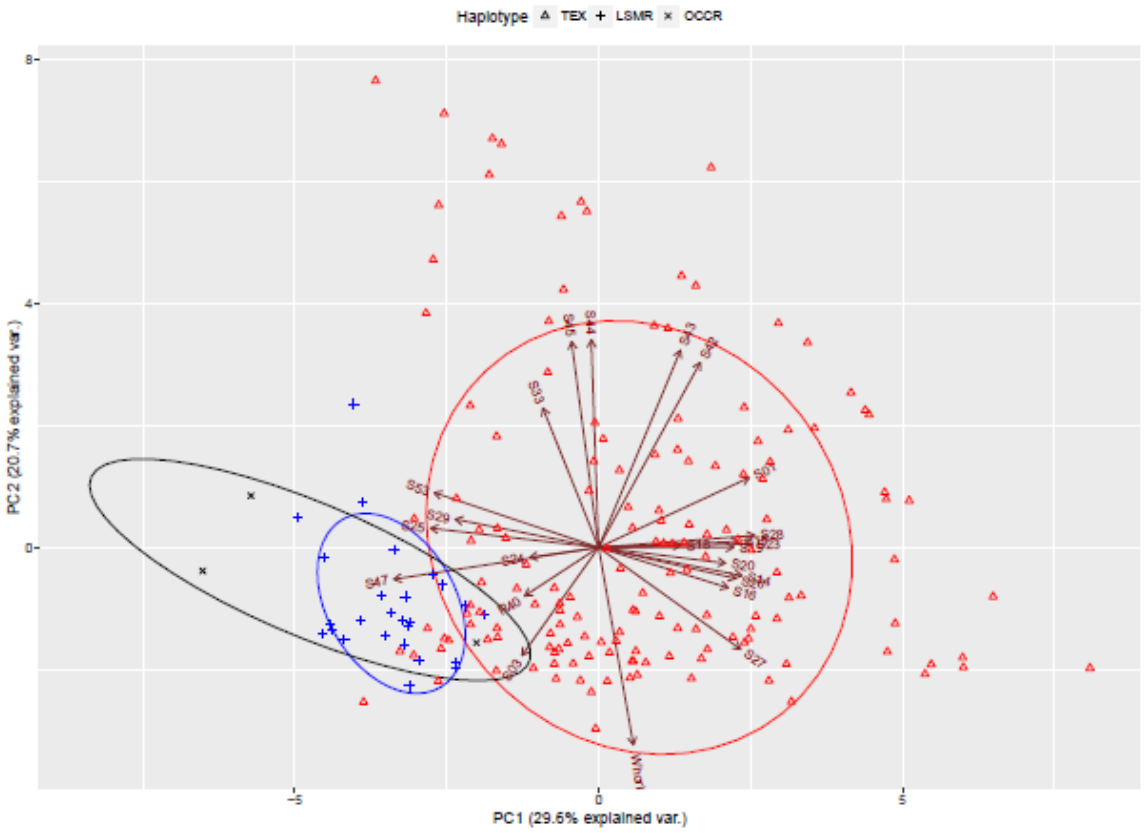

Figure 15: Principal Components Analysis plot showing haplotype clusters based on shell geometry estimates from the 24 retained variables. Analysis supports the assumption that the haplotypes differ in shell shape.

Linear Discriminant Functions Analysis

LDF analysis results based on the 46 morphometric variables tested indicate three distinct clusters of snails corresponding to haplotype (Figure 16). Among the 46 variables used for discrimination the variables: $\frac{W_B}{L_{B+2}}$, $\frac{W_B}{L_B}$, and $\frac{L_B}{L_{B+2}}$ are the strongest discriminants followed by $\frac{W_{Whl\#6}}{L_T}$, $\frac{L_{Whl\#6}}{L_T}$, $\frac{W_{(n-2)b}}{W_{(n-1)b}}$, $W_{Whl\#6}$, and $L_{Whl\#6}$ (See Table in TABLES section for coefficients of linear discriminants). The percentage of snail

separation achieved by LD1 is 85.25% and LD2 is 14.75%. The LDF analysis of quantitative variables reliably predicts haplotype (Table in the TABLES section).

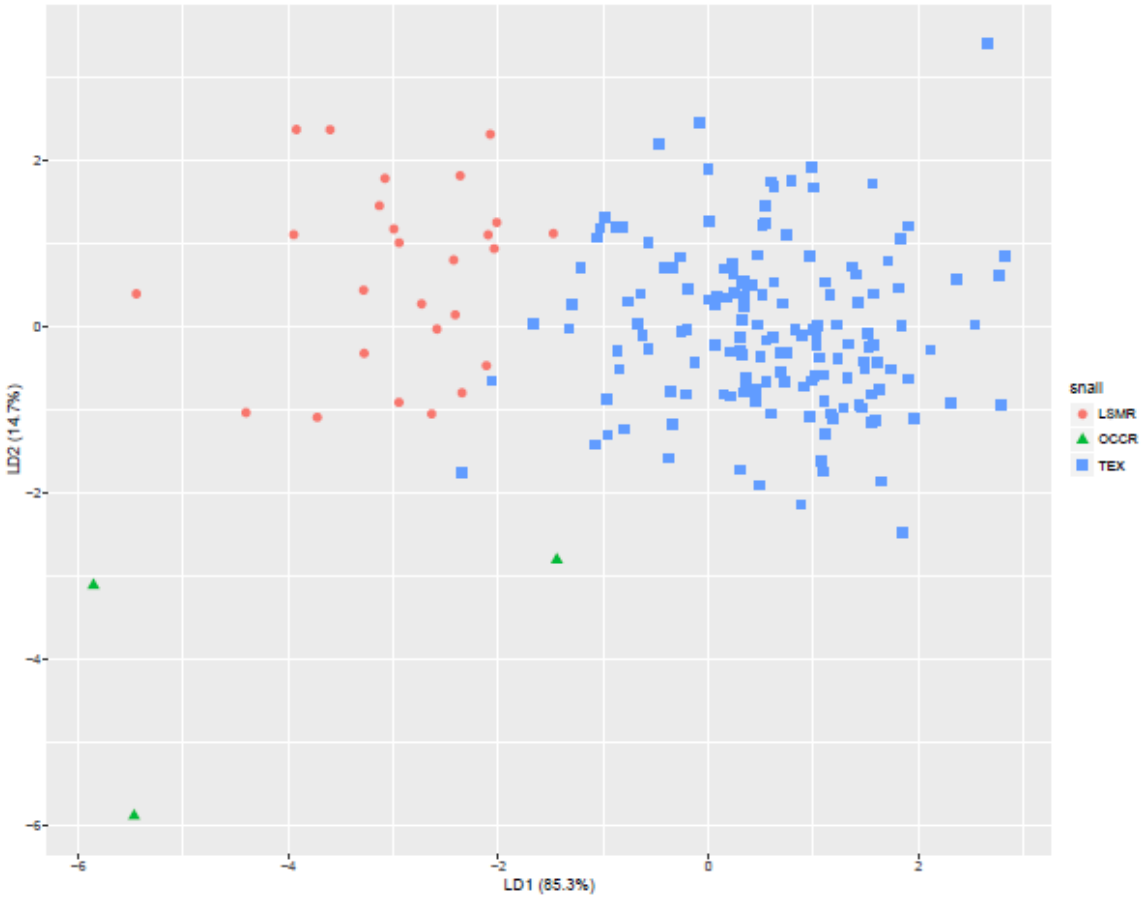

Figure 16: (Left) Plot of Linear Discriminant Functions visualizing clusters using shell morphometric variables as related to haplotype. LDF plot supports differences in shell shape geometry that is associated with haplotype.

IV. DISCUSSION

Current Distributional Status of *M. tuberculata* in Central Texas

Results of this study now serve as an update to known ranges and habitat associations for *M. tuberculata* in central Texas. Based on the results of these analyses, it is reasonable to assume there are indeed different physiological tolerances among the different haplotypes detected in this study and assumptions of restrictions to thermally stable environments are no longer valid, at least for some haplotypes. The fact that there only haplotype detected in the thermally ambient reaches of the lower San Marcos River supports these assumptions. It would also seem reasonable to assume that snails found in the Upper San Marcos River have no restrictions to colonization of the lower thermally ambient reaches other than inherent differences in physiological differences among the different haplotypes. However, more research is needed to conclusively establish differences in lethal thermal minima among the different haplotypes.

With respect to previously reported *Melanoides sp*. in the Guadalupe River, phenotypic and genetic identities remain unknown. The detection of the LSMR haplotype and three individuals of the rare OCCR haplotype in the Old Channel of the Comal River may provide insight to previous observations of range expansion in the Guadalupe River. It is possible that the snails observed in the thermally ambient stretches of the Guadalupe River may have belonged to these rare haplotypes. Continued monitoring is recommended for the Guadalupe River.

Additionally, it would be reasonable to assume that the occurrence of *M. tuberculata* in thermally ambient reaches of the San Marcos River is not an anomaly. A

reasonable hypothesis is that there are more thermally ambient environments throughout Texas and indeed, the United States, that contain overlooked populations of *M. tuberculata*. More sampling is needed to evaluate this hypothesis.

Molecular Analyses

Molecular results of this study support previous work establishing *M. tuberculata* as polyphyletic and highly diverged. It is an interesting observation that the TEX haplotype, although identified as *M. tuberculata* by previous studies, appears to be more closely related to *Melanoides amabilis* than to other *M. tuberculata* analyzed in this study. Additionally, there is little evidence in the literature that supports exclusivity of the *M. tuberculata* species in general. During literature review for this project, there was difficulty finding and obtaining taxonomic diagnostics for the family Thiaridae. In light of recent studies establishing genetic relationships among the different populations of thiarids, future work could include consolidation of taxonomic data, possible reassessment and revision of the *Melanoides* genus.

With respect to phylogenetic relationships, it is possible that the arbitrarily named haplotypes observed in this study in fact belong to one of the haplotypes found globally. However, all of the previously published works characterizing the morphology and genetic identity of the closely aligned haplotypes did not provide photographic evidence of all the haplotypes reported and only provided cryptic morphological references to these snails. Furthermore, the limited length base pairs for the 16S rRNA region of mitochondrial DNA amplified could be interpreted as providing little resolving power of observed genetic similarity or possible dissimilarity. It is my opinion that in order for

conclusive relationships to be established, a mitochondrial genome perspective is warranted and will be the future direction of my work.

It is worth noting that sequencing of other regions of DNA, both nuclear (microsatellites and ITS regions) and mitochondrial DNA (CO1 and 12S rRNA), were attempted during the course of this study. However, even though primer sequences proven to be successful in previously published work were used, differences in successful amplification were observed among the snails. For example, amplification of the 16S rRNA region of the mitochondrial genome was successful but amplifying the COI region consistently was not. This alludes to potential variability in binding locations among the snails used in this study. Sequencing of ITS regions of the nuclear genome was successful; however there was strong evidence of polyploidy interference in the sequence chromatograms making their interpretation unreliable.

Morphometric Analyses

Qualitative analysis

It is reasonable to assume that phenotypic assessments of genetic identity are not advisable for the TEX haplotype unless all unique phenotypes can be reliably associated with a genotype. The usage of inherently plastic morphological characters to serve as the foundation of identity is, in my opinion, fallacious and not likely to withstand rigorous criticism. A majority of the TEX haplotype snails collected in this study could not be definitively separated on phenotypic characters alone. Analyses were confounded by the presence of environmentally induced obstructions to assessing conch morphology. Heavy calcification was a common occurrence among collected snails. This and other

natural obstructions made it difficult to include many snails in the morphological analyses. This suggests that more robust techniques of phenotypic assessment are needed.

The TEX haplotype can be qualitatively characterized as having pale to dark background coloration, variable ornamentation patterns, may or may not have a columellar band, a diffuse to thick columellar band (when present), and a broad range of shell sculpture patterns. The LSMR haplotype can be qualitatively characterized as have a very pale, tan shell with green undertones, variable ornamentation patterns that are always small or narrow in size, generally lacks a columellar band, a narrow or diffuse columellar band (when present), deep U shaped spiral grooves with reticulate patterns in the grooves, and generally lacks axial ribs (but very mild and shallow when present). The OCCR haplotype can be qualitatively characterized as having medium to dark, brown to reddish brown background coloration, dense flames over spots ornamentation patterns, a thick columellar band, deep U shaped spiral grooves with reticulate patterns in the grooves, flat spiral ridges bordering the grooves, and deep prominent axial ribs.

Despite showing overlap in characteristics, there were some distinct phenotypic patterns observed among the collected snails. Genotyping experiments on Texas snails, using approaches similar to those carried out by Samadi et al. (1999) may be able to associate definitive genetic identities with phenotypes within the TEX haplotype that are otherwise not immediately differentiable. Based on the consistency of exhibited qualitative characters within the LSMR and OCCR haplotypes, these haplotypes do not show the wide range of phenotypic variability observed in the TEX haplotype.

Quantitative Analysis

Multivariate analyses did support phenotypic dissimilarity among the haplotypes and definitive clusters were observed in geometrical estimates of conch morphology. The usage of PCA is questionable in this study because the KMO measure of sample adequacy did not meet the generally accepted criteria. However, with a larger sample size this does not become a concern and PCA could be a viable option. This dataset could be built upon and the utility of PCA could prove useful in future studies. LDF analysis proved to be the more robust estimator of shell variable utility and was the more powerful technique for our data set.

It is worth asking if shell geometry alone is enough to estimate real morphological variation in *M. tuberculata*. Plasticity of shell geometry has been observed in previous studies and therefore can be misleading. Significant differences in the shell shape of two perceived morphotypes of *Physa sp*. were demonstrated to breakdown within two generations from being removed from environmental factors (Gustafson *et al*., 2014). Other common garden experiments have demonstrated that morphological characters not detected on wild caught individuals of *M. tuberculata* will manifest in F1 individuals (Van Bocxlaer *et al*., 2015). However, it was not known if the F1 individuals from that study were products of sexual reproduction or parthenogenesis alone. Multiple generations of lab bred individuals that are removed from the possibility of genetic variability due to sexual reproduction are needed before definitive conclusions on conch character plasticity can be made.

Results from this study stands to provide some basis for using phenotype as an indicator for genetic dissimilarity but the snails included in this study have failed to be

put through the rigors of common garden assessment. It is recommended that the different haplotypes found in this study be subjected to common garden experimentation before the observed acute phenotypic dissimilarity between haplotypes can be reliably used in the future.

V. CONCLUSIONS

Inherent differences in physiological limits rooted by observed divergences in genetic distance are suspected to be the factor leading to range expansion of *M. tuberculata* within the San Marcos River. It would appear that there have been multiple introduction events of *M. tuberculata* into central Texas waters. This is supported by observed phylogenetic relationships. The TEX haplotype falls into the southern Asian clade and is likely to have originated from that region of the world. The LSMR and OCCR haplotypes fall into the African and Asian clade and are likely of African descent. It is possible that these haplotypes originated from the Asian continent, however due to the similarity in genetic identity to other African lineages, it is not expected. Comparing these two haplotypes with other Melanids of Asian descent are needed to further support this hypothesis. Due to the large observed genetic divergence among the three haplotypes, it is not likely that the LSMR or OCCR haplotypes evolved within the San Marcos and Comal rivers.

The range expansion of *M. tuberculata* is of concern due to the fact that this species of snail serves as an intermediate host for broad range of parasitic species, some of which infect humans. It is expected that these parasites will inevitably follow their snail hosts into new and novel habitats. This study serves as the first official report of *M. tuberculata* establishment into surface-fed, thermally ambient habitats in the United States.

TABLES

Table 1: Modified Qualitative data matrix displaying 14 shell characteristics and unique phenotypes relative to river system.

River Phenotype	Background Color		Ornamentation			Columellar Band		Sculptures						
	IN	TI	DO	OT	SO	CB	CBT	GR	SR	SH	AR	RH	RT	RD
CR	3	1	1	4	1	0		0			1	2	1	1
CR	2	1	2	4	1	0		0			0			
CR	3	3	0			0		0			1	1	3	3
CR	3	3	1	2	1	0		0			1	2	2	2
CR	3	4	3	3	2	1	4	3	2	1	1	1	3	3
CR	3	6	3	4	2	1	3	2	3	1	1	2	1	1
CR	1	5	3	1	1	1	2	3	3	1	1	1	1	1
CR	3	3	3	3	1	1	4	3	2	1	1	1	3	3
CR	3	1	3	1	2	1	4	2	3	1	1	2	1	1
CR	3	6	3	1	3	1	4	2	3	1	1	2	1	1
CR	3	4	3	1	3	0		2	3	2	1	2	2	2
CR	3	4	4	3	3	1	4	2	1	2	1	2	2	1
CR	3	2	2	3	2	0		2	3	3	1	1	2	2
CR	3	2	3	3	3	1	1	3	2	1	1	1	2	2
CR	2	1	3	3	3	0		3	2	1	0			
CR	3	2	1	5	1	0		1	1	2	1	2	2	2
CR	2	2	2	5	3	0		1	1	2	1	2	2	2
CR	2	2	2	5	1	0		1	1	2	1	2	1	1
CR	2	2	2	5	1	1	1	2	2	1	1	2	1	1
CR	2	2	2	5	2	0		2	2	1	1	2	1	1
SFS	3	2	3	3	3	1	4	2	3	1	1	2	2	1
SFS	2	6	2	3	2	1	4	2	3	1	0			
SFS	2	2	3	3	2	1	4	2	3	1	0			
SFS	3	6	3	4	2	1	4	2	1	1	1	1	2	1
SFS	3	2	2	4	3	1	4	2	3	1	0			
SFS	3	6	3	3	3	1	4	2	3	1	1	2	2	1
SFS	3	2	2	3	2	1	4	2	3	1	1	2	2	1
FinSp	3	6	3	4	2	1	1	2	1	1	0			
FinSp	3	3	3	1	3	1	4	2	3	1	1	1	2	1
FCS	3	3	3	3	3	1	3	2	3	2	0			
FCS	3	3	3	1	3	1	3	2	3	1	1	2	2	1
FCS	3	6	2	4	3	1	4	2	1	1	1	2	2	1

Table 1 Continued: Modified Qualitative data matrix displaying 14 shell characteristics and unique phenotypes relative to river system.

FCS	3	6	3	1	3	1	4	2	3	1	1	2	2	1
FCS	3	6	3	1	3	1	4	2	3	1	0			
FCS	3	3	3	4	3	1	1	2	3	1	1	2	2	1
FCS	3	2	1	5	1	1	1	0		1	1	2	3	1
FCS	3	2	1	5	2	1	1	2	3	1	1	2	2	1
FCS	1	6	2	3	2	1	1	1	2	1	1	2	2	1
FCS	2	6	2	3	2	1	1	1	2	1	1	1	3	3
FCS	2	6	2	3	2	1	2	1	2	2	1	2	2	1
SMR	3	2	1	5	1	1	2	2	1	1	0			
SMR	2	1	3	1	2	1	4	4	3	1	0			
SMR	1	1	3	3	2	1	3	2	3	1	1	1	1	1
SMR	1	5	1	4	1	0		4	3	1	0			
SMR	1	5	2	3	1	0		3	3	1	0			
SMR	3	3	2	3	2	0		2	3	1	1	1	2	1
SMR	3	3	0			0		2	2	1	1	2	2	1
SMR	3	1	3	3	2	1	4	2	3	1	1	2	2	1
SMR	3	4	1	4	2	0		2	2	2	1	2	2	1
SMR	1	6	2	3	1	1	2	4	3	1	0			
SF	2	7	1	3	2	1	1	2	2	2	1	2	2	2

IN = Intensity of shell background color: (1) Very pale; (2) Pale; (3) Medium; (4) Dark

TI = Background shell color: (1) Amber; (2) Brown; (3) Dark Brown; (4) Red – Brown; (5) Tan w/ Green hue; (6) Green; (7) Gray

DO = Shell Ornamentation Density: (0) None; (1) Sparse; (2) Medium; (3) Dense

OT = Type of Shell Ornamentation: (1) Flames only; (2) Flame near apex; (3) More Flames than Spots; (4) More Spots than Flames; (5) Spots along the suture

SO = Relative Size of Ornamentation: (1) Small/Narrow; (2) Medium; (3) Large/Wide

CB = Presence of a Columellar Band: (0) No; (1) Yes

CBT = Thickness of Columellar Band (if present): (1) Diffuse; (2) Narrow; (3) Medium; (4) Wide

GR = Spiral Grooves: (0) Absent; (1) Shallow V shaped grooves; (2) Shallow U-shaped grooves; (3) Deep U shaped grooves; (4) Deep U shaped grooves with reticulation

SR = Type of Ridges bordering Spiral Groove: (1) Smooth; (2) Flat Ridges; (3) Pointed Ridges

SH = Spiral Groove Heterogeneity: (1) Homogeneous; (2) Heterogeneous among whorls; (3) Heterogeneous within whorl

AR = Presence of Axial Ribs: (0) Absent; (1) Present

RH = Axial Rib Heterogeneity: (1) Homogeneous; (2) Heterogeneous

RT = Thickness of Axial Rib: (1) Very mild; (2) Mild; (3) Prominent

RD = Depth of Axial Rib: (1) Shallow; (2) Medium; (3) Deep

Blank values indicate lack of character exhibition

Table 2 List of variables and corresponding variable loadings for the first four components of the Principal Components Analysis.

Variables	Loadings			
	Comp 1	Comp 2	Comp 3	Comp 4
Whorls	0.058	-0.391	0.080	-0.067
R40	-0.123	-0.096	-0.264	-0.108
S01	0.250	0.138	0.236	0.015
S03	-0.127	-0.214	-0.082	0.293
S14	0.238	-0.056	-0.110	0.476
S15	0.233	0.012	0.180	-0.070
S16	0.215	-0.080	0.121	-0.088
S18	0.136	0.004	-0.462	0.068
S19	0.224		-0.096	-0.196
S20	0.210	-0.031	-0.073	-0.380
S23	0.253	0.007	-0.271	-0.293
S24	-0.114	-0.020	0.461	-0.032
S25	-0.279	0.038	-0.023	-0.264
S26	0.228	-0.061	0.286	-0.103
S27	0.236	-0.201	0.139	-0.087
S28	0.259	0.024	-0.319	-0.209
S29	-0.238	0.056	0.110	-0.476
S33	-0.092	0.276	-0.070	-0.032
S42	0.169	0.366	0.141	0.009
S43	0.136	0.390	0.130	0.029
S44	-0.012	0.411	-0.059	0.044
S45	-0.045	0.407	-0.061	0.093

Table 2 Continued: List of variables and corresponding variable loadings for the first four components of the Principal Components Analysis.

S47	-0.340	-0.063	0.041	-0.025
S53	-0.273	0.108	-0.148	-0.111

Table 3: Listed below are the coefficients of linear discriminants obtained from linear discriminant functions analysis.

Variable	LD1	LD2
Whorls	-1.29583194	-0.59506076
R40	-0.10166921	-0.58857167
S01	-0.12431050	-0.39467798
S02	-0.29948327	-0.14545362
S03	3.68113602	-1.21471720
S04	-2.80999135	1.20155958
S05	-3.65766124	2.01943005
S06	0.65309276	0.98407324
S07	3.89723056	-1.71272452
S08	2.01740089	-1.83441398
S09	-1.35825272	0.02405143
S10	-0.97234681	0.76336437
S11	-2.15765720	-3.82504236
S12	-2.20729342	0.74757830
S13	-0.76170518	0.86535251
S14	-0.22473690	0.62809124
S15	-6.15060814	-1.01858680
S16	-2.13953849	-1.53835056
S17	-1.04976699	-1.06131986
S18	-1.18063453	0.07851682
S19	1.12503455	-3.75354318
S20	-1.86321649	-0.94490589
S21	-3.29537390	1.13428982
S22	1.84710576	-1.27157982
S23	-1.20580698	-1.61627093
S24	0.41236797	-0.32900295
S25	-0.01008631	0.11871513
S26	-1.99437769	0.99291945
S27	4.82576509	-0.16333589
S28	3.07879959	4.17833084
S29	0.22473690	-0.62809124
S33	2.61957850	0.14701007
S34	-0.72951739	2.65273844
S35	-3.64477342	-2.06443064
S36	-0.20792679	-2.01697578
S37	-0.60451074	-0.84309229

Table 3 Continued: Listed below are the coefficients of linear discriminants obtained from linear discriminant functions analysis.

S38	-0.65309276	-0.98407324
S42	5.94911793	4.17622890
S43	-5.22417327	-4.61369317
S44	-3.03318663	-6.58041642
S45	1.39730711	7.08850677
S46	0.01298830	0.92337575
S47	14.48054706	23.32766317
S48	-12.67459457	-21.27918167
S49	-7.56121559	-12.57887377
S50	-0.65070738	0.40248808
S51	0.77130759	-0.92696306
S52	-0.78726842	0.75380946
S53	1.28166624	-0.61069040

Table 4: Accuracy of LDF haplotype prediction based on morphometric variables. The numbers in the matrix represent the number times the LDF analysis predicted haplotype identity based on the geometric estimates of shell shape. An incorrect prediction can be observed by misalignment in the matrix. For example, the analysis predicted the LSMR haplotype correctly 25 out 26 instances.

	TEX	LSMR	OCCR
TEX	152	1	1
LSMR	2	25	0
OCCR	0	0	2

APPENDIX SECTION

Table 5: A list of rivers, associated sampling locations and corresponding gps coordinates

Collection Locality	Sample Site	GPS Coordinate
Comal River	Upper Spring Run	29.720508, -98.128588
	USR Enclosures	29.718802, -98.13047
	New Channel	29.708152, -98.132728
	LL Dam	29.710627, -98.134565
	LL Dock	29.711799, -98.13555
	Island Above Spring Island	29.718249, -98.131273
	Spring Island	29.717672, -98.132243
	Old Channel	29.712215, -98.128413
San Marcos River	SMR1	29.889436, -97.934391
	SMR2	29.882381, -97.934947
	SMR3	29.880031, -97.932736
	SMR4	29.876614, -97.931744
	SMR5	29.868969, -97.928458
	SMR6	29.871281, -97.915633
	SMR7	29.857239, -97.896806
	SMR8	29.849542, -97.856864
	SMR9	29.782072, -97.830600
	SMR10	29.752686, -97.780914
	SMR11	29.728031, -97.760786
	SMR12	29.716842, -97.753125
	SMR13	29.711983, -97.737881
	SMR14	29.667508, -97.699619
	SMR15	29.665936, -97.650653
	SMR16	29.590725, -97.584297

Table 5 Continued: A list of rivers, associated sampling locations and corresponding gps coordinates

San Felipe River	HWst5	29.373619, -100.885169
	CSSt1	29.369194, -100.884792
	MSt3	29.367644, -100.88395
Finnegan Springs	Unnamed Locality	29.900014, -100.998144
Las Moras Springs	Head Waters	29.309861, -100.42125
	Spring Pool	29.309311, -100.421508
	Creek Below Guard House	29.307478, -100.417542

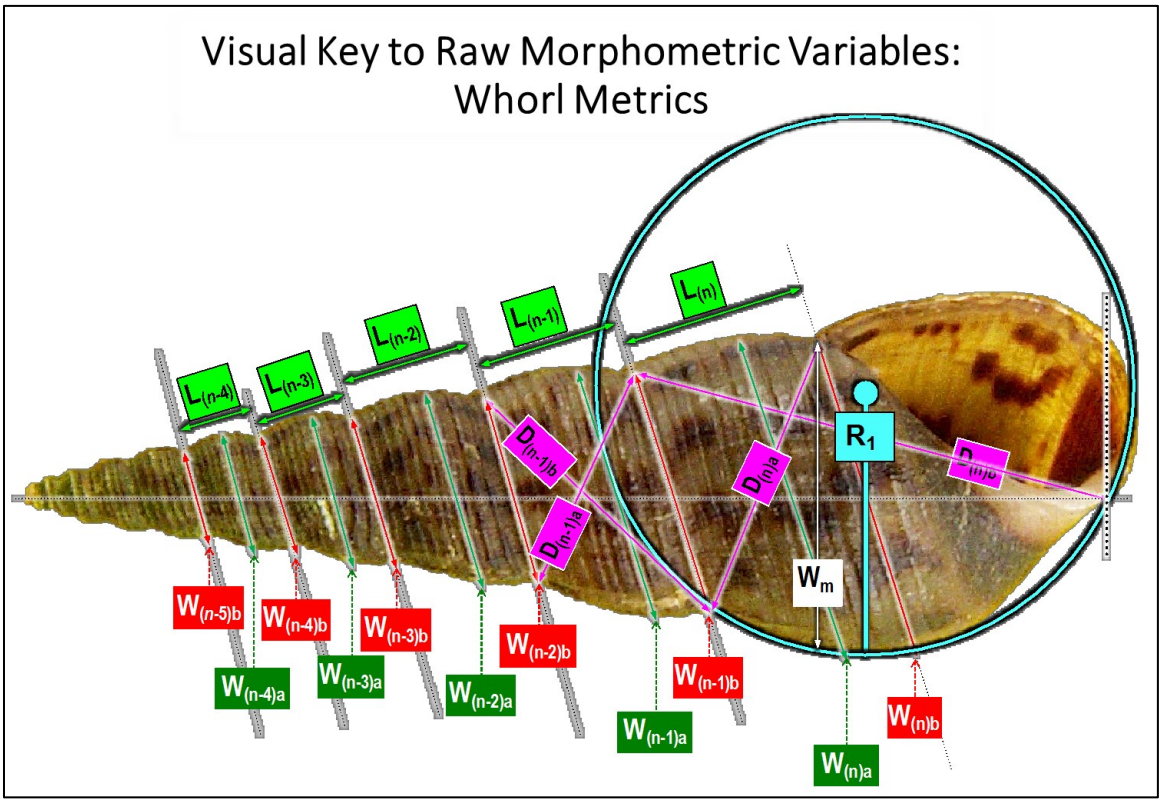

Figure 17 Image visualizing whorl metric variables from the raw morphometric variable set. Code names and definitions for these variables can be located in **Table** .

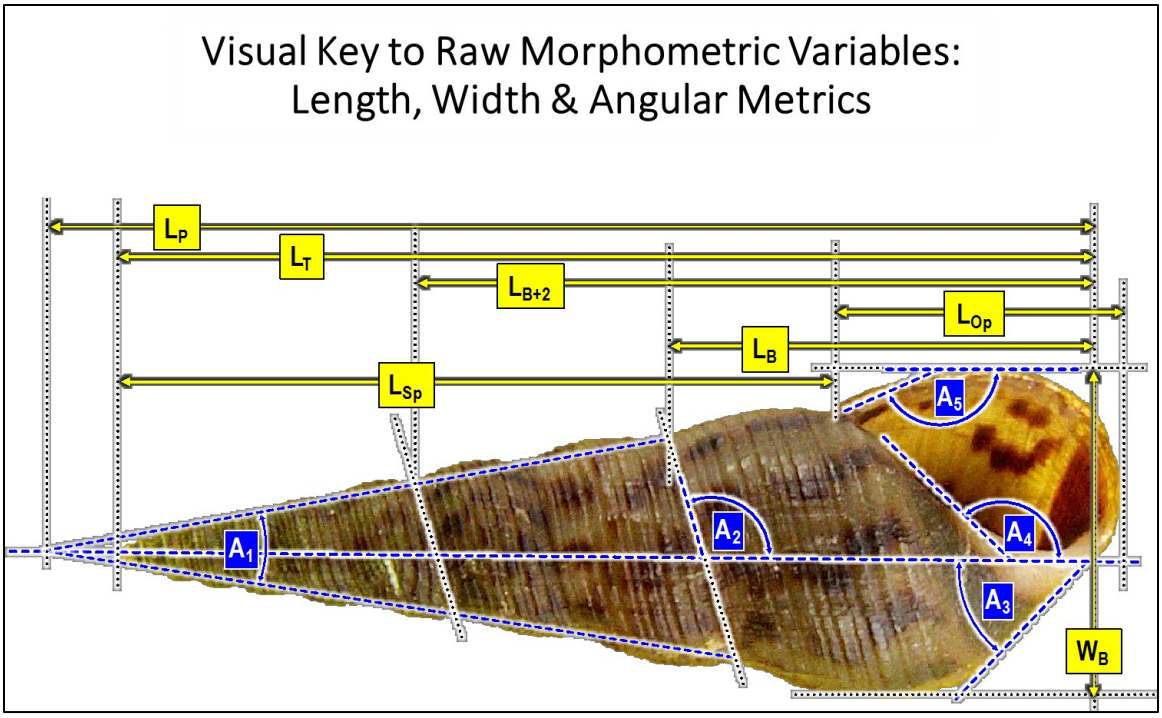

Figure 18: Image visualizing length, width and angular metric variables from the raw morphometric variable set. Code names and definitions for these variables can be located in **Table**

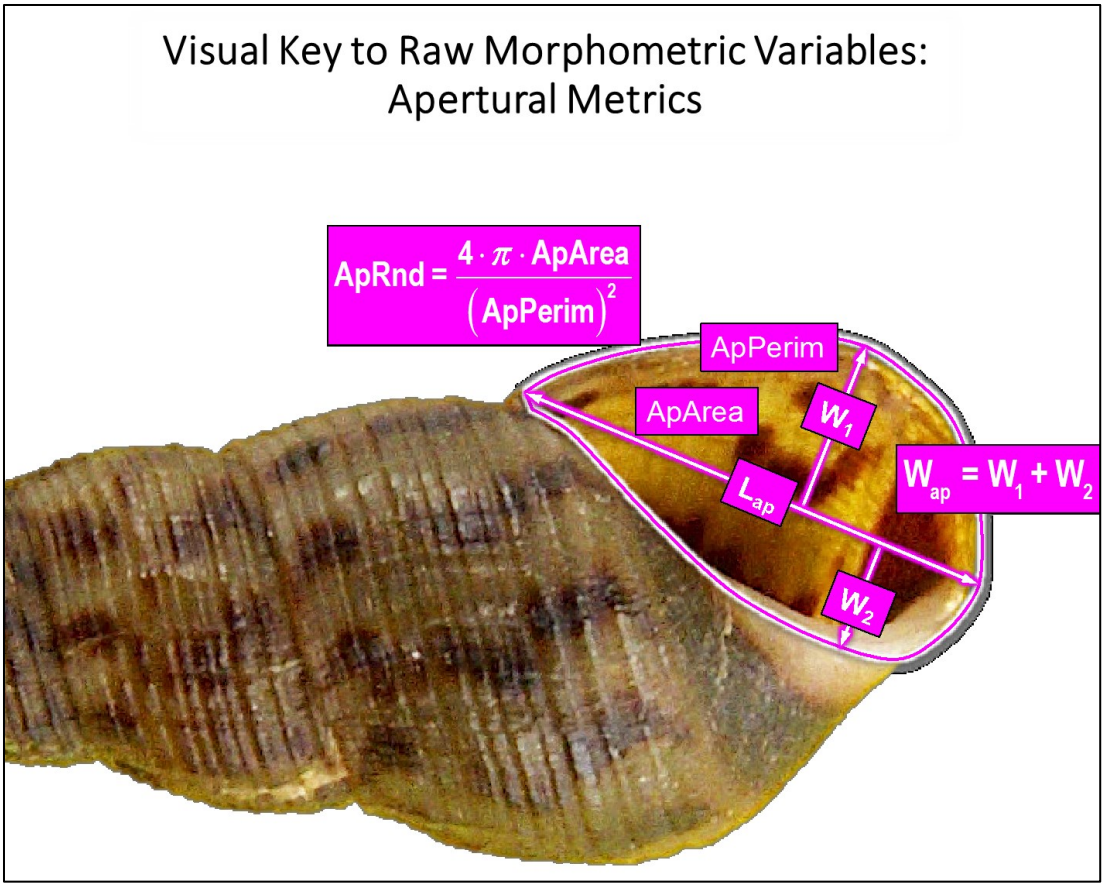

Figure 19: Image visualizing apertural metric variables from the raw morphometric variable set. Code names and definitions for these variables can be located in **Table**

Table 6: List of variable codes, variable names, and associated definitions.

Variable Code	Variable Name	Variable Definitions
R01	Whorls	Counted (or estimated) number of whorls (n).
R02	Lt	Length end-to-end for intact specimens.
R03	Lp	Projected length, based on the convergence of two lines posteriad, with line angles determined by last three sutures on opposite sides.
R04	LB	Body Length; distance parallel to columellar axis from dextral end of penultimate $(n-1)^{th}$ suture to a line perpendicular to the columellar axis and across extreme anterior end of aperture lip.
R05	LB+2	Same as BL, except extended two more whorls to dextral end of $(n-3)^{th}$ suture.
R06	LSp	Length of Spire (from opercle to tip).

Table 6 Continued: List of variable codes, variable names, and associated definitions.

R07	LOp	Length of opercular opening, as measured parallel to body axis.
R08	WM	Diameter at anal sulcus, perpendicular to body axis.
R09	WB	Maximum width of body perpendicular to body axis.
R10	L(n)	Thickness of body (ultimate, n^{th}) whorl.
R11	L(n-1)	Thickness of penultimate $(n-1)^{th}$ whorl.
R12	L(n-2)	Thickness of antepenultimate $(n-2)^{th}$ whorl.
R13	L(n-3)	Thickness of $(n-3)^{th}$ whorl.
R14	L(n-4)	Thickness of $(n-4)^{th}$ whorl.
R15	W(n)b	Distance from last sutural groove near aperture to opposite side of body (ultimate, nth) whorl, measured parallel to sutures with aperture up.
R16	W(n)a	Maximum distance across body (ultimate, n^{th}) whorl, measured parallel to sutures.
R17	W(n-1)b	Minimum distance across penultimate suture, measured across base of body (ultimate, nth) whorl with aperture up.
R18	W(n-1)a	Maximum distance across penultimate $(n-1)^{th}$ whorl, measured parallel to sutures.
R19	W(n-2)b	Minimum distance across antepenultimate $(n-2)^{th}$ suture, measured parallel to sutures.
R20	W(n-2)a	Maximum distance across antepenultimate $(n-2)^{th}$ whorl, measured parallel to sutures.
R21	W(n-3)b	Minimum distance across $(n-3)^{th}$ suture, measured parallel to sutures.
R22	W(n-3)a	Maximum distance across $(n-3)^{th}$ whorl, measured parallel to sutures.
R23	W(n-4)b	Minimum distance across $(n-4)^{th}$ suture, measured parallel to sutures.
R24	W(n-4)a	Maximum distance across $(n-4)^{th}$ whorl, measured parallel to sutures.
R25	W(n-5)b	Minimum distance across $(n-5)^{th}$ suture, measured parallel to sutures.
R26	D(n)a	Diagonal distance across body (ultimate, nth) whorl from dextral groove of last (ultimate, nth) suture near aperture (with aperture up) to opposite (sinistral) end of penultimate $(n-1)^{th}$ suture.
R27	D(n)b	Distance from dextral groove of penultimate suture to anterior-most end of columella.
R28	D(n-1)a	Diagonal distance from dextral end of penultimate $(n-1)^{th}$ suture to sinistral end of antepenultimate $(n-2)^{th}$ suture.

Table 6 Continued: List of variable codes, variable names, and associated definitions.

R29	D(n-1)b	Diagonal distance from dextral end of antepenultimate $(n-1)^{th}$ suture to sinistral end of penultimate $(n-1)^{th}$ suture.
R30	A1	Acute angle between two lines tangent to the grooves of the largest three whorls of the shell, converging at the columellar axis posteriorly (apex determines LP).
R31	A2	Obtuse angle between the penultimate $(n-1)^{th}$ suture and the columellar axis.
R32	A3	Acute angle between the columellar axis and a line tangent to the sinistral edge of the shell opposite the aperture between the extreme anterior end of the columella and the sinistral bulge of the body whorl.
R33	A4	Obtuse angle between the columellar axis and a line along the parietal wall of the aperture.
R34	A5	Obtuse angle representing the curvature of the lip back towards the sulcus.
R35	R1	Radius of curvature of the sinistral margin of the body whorl.
R36	ApArea	Aperture area as determined by the AREA function of Digimizer (outline determined by limits of nacre).
R37	ApPerim	Aperture perimeter as determined by the AREA function of Digimizer (outline determined by limits of nacre).
R38	LAp	Aperture Length, as determined by the AREA function of Digimizer (the maximum distance between any two points in the perimeter).
R39	WAp	Aperture width, as determined by the AREA function of Digimizer (establishes a line representing LAp, and then sums the maximum distances between the line and the most distant points either side of the line).
R40	ApRnd	Index of "roundness" of the apertural opening (4*Pi*Area), such that a perfectly round opening would have an index value of 1.0, and very unround margins would yield a value approaching zero.

REFERENCES

Abbott RT. 1973. Spread of Melanoides tuberculata. Nautilus 87.1: 29.

Benson AJ, Neilson ME. 2015. USGS - NAS - Nonindigenous Aquatic Species: Melanoides tuberculatus. http://nas.er.usgs.gov/queries/FactSheet.aspx?SpeciesID=1037 Revision Date: 2/28/2013 Accessed 2015

Boc A, Diallo AB, Makarenkov V. 2012. T-REX: a web server for inferring, validating and visualizing phylogenetic trees and networks. Nucleic Acids Research, 40(Web Server issue), W573–W579. http://doi.org/10.1093/nar/gks485.

Facon B, Pointier JP, Glaubrecht M, Poux C, Jarne P, David P. 2003. A molecular phylogeography approach to biological invasions of the New World by parthenogenetic thiarid snails. Mol Ecol 12:3027-3039

Fleming BP. 2002. Downstream spread of the digenetic trematode Centrocestus formosanus, into the Guadalupe River, Texas. MS Thesis, Texas State University, San Marcos, TX

Genner MJ, Michel E, Todd JA. 2007. Resistance of an invasive gastropod to an indigenous trematode parasite in Lake Malawi. Biological Invasions 10:41-49

Gerald GW, Spezzano LC. 2005. The influence of chemical cues and conspecific density on the temperature selection of a freshwater snail (Melanoides tuberculata). Journal of Thermal Biology 30:237-245. doi: DOI: 10.1016/j.jtherbio.2004.12.002

Gustafson KD, Kensinger BJ, Bolek MG, Luttbeg B. 2014. Distinct snail (Physa) morphotypes from different habitats converge in shell shape and size under common garden conditions. *Evolutionary Ecology Research*, *16*(1), 77–89.

Haseeb MA, Fried B. 1997. Modes of transmission of trematode infections and their control. In: Fried B, Graczyk TK (eds) Advances in Trematode Biology, 1st edn. CRC Press, pp 480

Huelsenbeck JP, Ronquist F. 2001. MRBAYES: Bayesian inference of phylogeny. Bioinformatics 17:754-755.

Jacob J, 1958. XVI.--Cytological studies of Melaniidæ (Mollusca) with special reference to parthenogenesis and polyploidy. I. Oögenesis of the parthenogenetic species of Melanoides (Prosobranchia-Gastropoda). Transactions of the Royal Society of Edinburgh 63: 341-352

Karatayev AY, Burlakova LE, Karatayev VA, Padilla DK. 2009. Introduction, distribution, spread, and impacts of exotic freshwater gastropods in Texas. Hydrobiologia 619:181-194. doi: 1O.1007/s10750-008-9639-y

Kearse M, Moir R, Wilson A, Stones-Havas S, Cheung M, Sturrock S, Buxton S, Cooper A, Markowitz S, Duran C, Thierer T, Ashton B, Mentjies P, Drummond A. 2012. Geneious Basic: an integrated and extendable desktop software platform for the organization and analysis of sequence data.Bioinformatics, 28(12), 1647-1649.

Lindholm JT. 1979. The Gastropods of the Upper San Marcos River and their Trematode Parasites. Master of Science, Texas State University, San Marcos, TX

Livshits G, Fishelson L. 1983. Biology and reproduction of the freshwater snail Melanoides tuberculata (Gastropoda: Prosobranchia) in Israel. Israel Journal of Zoology 32:21-35

Livshits G, Fishelson L, Wise GS. 1984. Genetic similarity and diversity of parthenogenetic and bisexual populations of the freshwater snail Melanoides tuberculata (Gastropoda: Prosobranchia). Biological Journal of the Linnean Society 23: 41-54

Miller MA, Pfeiffer W, Schwartz T. 2010 "Creating the CIPRES Science Gateway for inference of large phylogenetic trees" in Proceedings of the Gateway Computing Environments Workshop (GCE), 14 Nov. 2010, New Orleans, LA pp 1 - 8

Mitchell AJ, Brandt TM. 2005. Temperature tolerance of red-rim melania Melanoides tuberculatus, an exotic aquatic snail established in the United State. Transactions of the American Fisheries Society 134:126-131

Murray HD. 1964. Tarebia granifera and Melanoides tuberculata in Texas. Annual Report to the American Malacological Union 53:15-16

Murray HD. 1971. The introduction and spread of thiarids in the United States. Biologist 53:133-135

Murray HD. 1975. Melanoides tuberculata (Muller), Las Moras Creek, Bracketville, Texas. Bulletin of the American Malacological Union 42:43

Murray HD, Woopschall LJ. 1965. Ecology of Melanoides tuberculata (Müller) and Tarebia granifera (Lamarck) in South Texas. American Malacological Union Annual Reports 32:25-26

Perera G, Perera G, Ferrer JR, Arrinda C, Amador O. 1990. Effectiveness of three biological control agents against intermediate hosts of snail-mediated parasites in Cuba. Malacol Rev 23:47-52

Pinto HA, de Melo AL. 2011. A checklist of trematodes (Platyhelminthes) transmitted by Melanoides tuberculata (Mollusca: Thiaridae). Zootaxa 2799:15-28

Pointier JP. 1989. Conchological studies of Thiara (Melanoides) tuberculata (Mollusca: Gastropoda: Thiaridae) in the French West Indies. Walkerana 3:203-209

Pointier JP, Théron A, Borel G. 1993. Ecology of the introduced snail Melanoides tuberculata (Gastropoda- Thiaridae) in relation to Biomphalaria glabrata in the Marshy Forest Zone of Guadeloupe, French West Indies. Journal of Molluscan Studies 59:421-428

Rader RB, Belk MC, Keleher MJ. 2003. The introduction of an invasive snail (Melanoides tuberculata) to spring ecosystems of the Bonneville Basin, Utah. Journal of Freshwater Ecology 18:647-657

Samadi S, Mavarez J, Pointier JP, Delay B, Jarne P. 1999. Microsatellite and morphological analysis of population structure in the parthenogenetic freshwater snail Melanoides tuberculata: insights into the creation of clonal variability. Mol Ecol 8:1141-1153

Stamatakis, A. 2014. RAxML Version 8: A tool for Phylogenetic Analysis and Post-Analysis of Large Phylogenies. Bioinformatics 10.1093/bioinformatics/btu033 http://bioinformatics.oxfordjournals.org/content/early/2014/01/21/bioinformatics.btu033.abstract

Swofford DL. 2003. PAUP*. Phylogenetic Analysis Using Parsimony (*and Other Methods). Version 4. Sinauer Associates, Sunderland, Massachusetts

Thompson JD, Higgins DG, Gibson TJ. 1994. CLUSTAL W: improving the sensitivity of progressive multiple sequence alignment through sequence weighting, position-specific gap penalties and weight matrix choice. Nucleic Acids Research, 22(22), 4673–4680.

United States Geological Survey. Tarebia granifera. USGS Nonindigenous Aquatic Species Database, Gainesville, FL. United State Geological Survey (USGS). 2015. http://nas.er.usgs.gov/queries/FactSheet.aspx?SpeciesID=1039 2015

Van Bocxlaer B, Clewing C, Mongindo Etimosundja JP, Kankonda A, Wembo Ndeo O, Albrecht C. 2015. Recurrent camouflaged invasions and dispersal of an Asian freshwater gastropod in tropical Africa. BMC Evolutionary Biology, 15(1), 33. doi:10.1186/s12862-015-0296-2

Vaz JF, Teles HS, Correa MA, Leite SP. 1986. Ocorrência no Brasil de Thiara (Melanoides) tuberculata (OF Muller, 1774) (Gastropoda, Prosobranchia), primeiro hospedeiro intermediário de Clonorchis sinensis (Cobbold, 1875) (Trematoda, Plathyhelmintes). Rev Saúde públ 20:318-322

Wingard GL, Murray JB, Schill WB, Phillips EC. 2008 Red-rimmed melania (Melanoides tuberculatus) - A snail in Biscayne National Park, Florida - Harmful invader or just a nuisance?. U.S. Geological Survey, Reston, VA